ANALYSIS AND INTERPRETATION OF MEASUREMENTS FOR THE DETERMINATION OF ASBESTOS IN CORE SAMPLES COLLECTED AT THE SOUTHDOWN QUARRY IN SPARTA, NEW JERSEY

D. Wayne Berman, Ph.D.
Aeolus, Inc.
November 12, 2003

1 EXECUTIVE SUMMARY

As part of a study of exposure to and risk from potential emissions of asbestos from the Southdown Quarry (now Cemex), a series of rock core segments representing each of multiple depths were acquired from historical drill core samples of Quarry material provided by the quarry. The samples were then analyzed for the determination of asbestos and related structures. Results are summarized below along with an evaluation of the quality (reliability) of these measurements. Results are then interpreted to evaluate asbestos-related exposures and the attendant risks potentially associated with work at the quarry.

The New Jersey Department of Environmental Protection (NJDEP) and the U.S. Environmental Protection Agency (USEPA) in conjunction with the Environmental and Occupational Health Sciences Institute (EOHSI) of the University of Medicine and Dentistry of New Jersey, Rutgers University, and Aeolus, Inc. have been conducting an assessment of risks potentially posed by the putative presence of asbestos in marble mined at the Southdown Quarry in Sussex County, New Jersey. Operations at the quarry had initially attracted attention due to (1) the observed presence of tremolite in the marble mined at the quarry and (2) a report that tremolite asbestos structures were detected on an air conditioner filter at a residence located downwind of the quarry.

Analysis and evaluation of marble core samples represent the last phase of the multiphase study being conducted to evaluate asbestos-related risks potentially associated with operations at the quarry. Results of air and dust sampling in the vicinity of the quarry and at residences downwind of the quarry were previously reported (Lioy et al. 2002) and are accessible on the web (http://www.state.nj.us/dep/dsr/sparta/final-report.htm). Based on the measured concentrations of biologically relevant asbestos structures in air, those results indicate a small elevation in lifetime cancer risk of $2x10^{-6}$ – $3x0^{-5}$ (two-in-a million to three-in-a hundred thousand) for area residents, which is within the range generally considered *de minimus* and thus acceptable for purposes of air emissions permitting. The air and dust sampling results do not provide support for the hypothesis that the quarry was the source of the measured asbestos structures. However the data could not rule out the quarry as a possible source.

The issues to be addressed and the general approach to be adopted for the study of Southdown Quarry were first described in a detailed framework prepared by an expert panel assembled to oversee the study (Expert Panel-Commissioned by NJDEP/EPA 2000). For risk assessment, the approach proposed in a new protocol (Berman and Crump 2001) was adopted for this study.[1] In the new protocol, asbestos concentrations are determined by counting asbestos structures satisfying the dimensional criteria of a new exposure index[2] and cancer risk is assigned to the resulting exposure estimates using new exposure-response coefficients that are matched to the new index. The structures enumerated using this approach are henceforth referred to as "protocol structures."

The new approach was employed in parallel with the current USEPA approach for asbestos risk assessment. The current USEPA approach assigns risk to asbestos concentrations determined based on counts of structures that satisfy the "traditional" definition for fibers (Walton 1982), which are henceforth referred to as "7402 structures" (referring to the relevant NIOSH analytical method used to enumerate such structures). Under this approach, risk is assessed by multiplying estimated concentrations of 7402 structures by the current USEPA unit risk factor for asbestos (IRIS 1988).

Because the current approach assigns risk only to "true" asbestos *fibers* (while the Protocol Structure approach includes all mineralogically related structures of appropriate dimensions), a procedure developed by RJ Lee (the primary analytical laboratory for this study) was also employed to distinguish true asbestos fibers from cleavage fragments exhibiting similar mineralogy so that risks could be estimated with or without restricting exposure concentrations to true asbestos fibers.

A total of 15 samples representing composites of core segments from each of five archived drill cores were acquired for analysis. Core samples were identified and assessed for overall integrity by geologists from the NJDEP's New Jersey Geologic Survey. The composites were created by taking individual core segments from each respective core that represent the same specific depth interval and preparing them for analysis by splitting, crushing, combining, homogenizing, sieving, and sub-sampling. Sub-sampled splits were then analyzed per the Modified Elutriator Method (Berman and Kolk 2000).

---

[1] When the Framework was written, an older version of the new protocol (Berman and Crump 1999a and b) had been distributed for review. A revised version (Berman and Crump 2001) contains an updated review of the literature and a more sophisticated analysis of the available epidemiology data that better supports the approach proposed for risk assessment. Therefore, the newer document is cited throughout this report when referencing the protocol.

[2] An exposure index defines a specific range of structure sizes and shapes that are to be included in counts of structures used to determine asbestos concentrations.

Design objectives for the part of the Southdown study involving analysis of core samples were defined in the Quality Assurance Project Plan (EOHSI 2001) for the project. To assure that the quality of data derived from the analysis of core samples from the Southdown Quarry would satisfy the defined requirements, a range of QC analyses was performed.

Results of the QC analyses indicated that, with one exception, evaluation of the quality control data (blanks, replicates and duplicates) from this study showed good overall performance that achieved the quality objectives stated in the Quality Assurance Project Plan for this project (EOHSI 2001). Moreover, because the one exception involves inconsistent results among replicate analyses of a single sample and the source of the inconsistencies appear to be due to an isolated recording or characterization error by an analyst, the broader data set from this study should be considered generally useable to support their intended purpose.

The broader set of core concentration measurements was then used to evaluate risk. This was accomplished by:

- modeling emission and dispersion of dust from quarry operations to estimate airborne dust concentrations at locations where neighboring residents might become exposed[3];

- using measurements from the analysis of core samples to characterize the ratio of asbestos to respirable dust in the core material;

- applying the measured ratios of asbestos to dust in the bulk phase to the modeled airborne dust concentrations; and

- applying the appropriate dose-response factors to the estimated airborne asbestos concentrations to derive estimates of risk.

Evaluation of cancer risks resulting from lifetime exposure to neighboring residents posed by emissions of asbestos and related structures due to operations at the Southdown Quarry indicate that they are likely less than $1x10^{-5}$ (one-in-one-hundred-thousand), which is well within the risk range (of $1x10^{-4}$ to $1x10^{-6}$) that is generally considered acceptable by USEPA and the NJDEP (the latter for permitting of air emissions sources). Moreover, risks are projected to remain within this risk range for either existing or hypothetical future residents even as quarry operations continue into the future. Importantly, the risks estimated in this study remain acceptable whether cleavage fragments are included or excluded during determination of exposure.

---

[3] Due to the uncertainties inherent to modeling dust emissions and transport, conservative (maximum mean annual) estimates of modeled airborne PM_{10} concentrations were employed in the risk calculations.

Further, similar conclusions are reached whether risks are estimated based on concentrations of protocol structures or concentrations of 7402 structures. Finally, it is encouraging to note that the risks estimated in this evaluation are reasonably consistent with the estimates of risk based on air sampling. While the risks estimated from air sampling reflect risks extrapolated from current exposures, the risks estimated from the core samples better reflect long-term trends in exposure. Thus, the conclusions from the combined approaches indicate that there is little short or long-term risk to nearby residents attributable to asbestos exposure from operations at the quarry.

2 INTRODUCTION

As part of a study of exposure to and risk from potential emissions of asbestos from the Southdown Quarry (now Cemex), a series of rock core segments representing each of multiple depths were acquired from historical drill core samples of Quarry material provided by the quarry. The samples were then analyzed for the determination of asbestos and related structures. Results are summarized below along with an evaluation of the quality (reliability) of these measurements. Results are then interpreted to evaluate asbestos-related exposures and the attendant risks potentially associated with work at the quarry.

The New Jersey Department of Environmental Protection (NJDEP) and the U.S. Environmental Protection Agency (ISAPI) in conjunction with the Environmental and Occupational Health Sciences Institute (EOHSI) of the University of Medicine and Dentistry of New Jersey, Rutgers University, and Aeolus, Inc. have been conducting an assessment of risks potentially posed by the putative presence of asbestos in marble mined at the Southdown Quarry in Sussex County, New Jersey. Operations at the quarry had initially attracted attention due to (1) the observed presence of tremolite in the marble mined at the quarry and (2) a report that tremolite asbestos structures were detected on an air conditioner filter at a residence located downwind of the quarry.

Analysis and evaluation of marble core samples represent the last phase of the multiphase study being conducted to evaluate asbestos-related risks potentially associated with operations at the quarry. Results of air and dust sampling in the vicinity of the quarry and at residences downwind of the quarry were previously reported (Lioy et al. 2002) and are accessible on the web (http://www.state.nj.us/dep/dsr/sparta/final-report.htm). Based on the measured concentrations of biologically relevant asbestos structures in air, those results indicate a small elevation in lifetime cancer risk of $2x10^{-6}$ – $3x10^{-5}$ (two-in-a million to three-in-a hundred thousand) for area residents, which is within the range generally considered *de minimus* and thus acceptable for purposes of

air emissions permitting[4]. The air and dust sampling results do not provide support for the hypothesis that the quarry was the source of the measured asbestos structures. However the data could not rule out the quarry as a possible source.

Questions concerning whether future operations might pose a risk requires evaluation of the material to be quarried in the future. Moreover, direct analysis of source material (where concentrations of potentially hazardous materials would be highest) typically represents a more robust approach for identifying potential hazards (whether current or future) than sampling for hazardous substances after they have been diluted by dispersion in the environment. Therefore, core samples from the marble body of the quarry were sampled and analyzed and the results are presented in this report.

Importantly, estimating risks from soil or bulk measurements of asbestos requires that such measurements be combined with appropriately selected emission and dispersion models and these can introduce substantial uncertainty into the analysis. Nevertheless, especially given combination with bulk analytical results that are typically more robust than air measurements (see above), the overall limitations of this approach frequently compare favorably to those associated with extrapolating long-term risk from short-term, limited air (exposure) measurements.

3 BACKGROUND

The issues to be addressed and the general approach to be adopted for the study of Southdown Quarry were first described in a detailed framework prepared by an expert panel assembled to oversee the study (Expert Panel-Commissioned by NJDEP/EPA 2000). For risk assessment, the approach proposed in a new protocol (Berman and Crump 2001) was adopted for this study.[5] In this framework:

- asbestos was defined;
- the health effects associated with asbestos were identified;
- controversies concerning the relationship between true asbestos fibers and cleavage fragments of asbestos-related minerals were addressed;
- terminology suitable for addressing the relevant distinctions among fibrous structures was developed;
- considerations for measurement of asbestos were defined;
- procedures to be used for evaluating asbestos-related risks were specified; and

---

[4] Risks below this risk range (i.e. less than one-in-one-million) are uniformly considered to be below any level of concern.

[5] When the Framework was written, an older version of the new protocol (Berman and Crump 1999a and b) had been distributed for review. A revised version (Berman and Crump 2001) contains an updated review of the literature and a more sophisticated analysis of the available epidemiology data that better supports the approach proposed for risk assessment. Therefore, the newer document is cited throughout this report when referencing the protocol.

- an overall approach for the Southdown study was recommended.

Note that the issues addressed in the framework are important to the Southdown study because, among other things, while it is believed that the tremolite observed in the marble at the quarry is predominantly massive or acicular (as opposed to fibrous), it is not known whether at least a fraction of the tremolite is asbestiform (i.e. true asbestos).

To facilitate review of this report, a few of the most important considerations documented in the framework are summarized here.

3.1 The Definition of Asbestos

As indicated in Berman and Crump (2001), asbestos is a term used to describe the fibrous habit of a family of hydrated metal silicate minerals. The most widely accepted definition of asbestos includes the fibrous habits of six of these minerals (IARC 1977). The most common type of asbestos is chrysotile, which is the fibrous habit of the mineral serpentine. The other five asbestos minerals are all amphiboles (i.e. all partially hydrolyzed, magnesium silicates). These are: fibrous reibeckite (crocidolite), fibrous grunerite (amosite), anthophyllite asbestos, tremolite asbestos, and actinolite asbestos.

All six of the minerals whose fibrous habits are termed asbestos occur most commonly in non-fibrous, massive habits. While unique names have been assigned to the asbestiform varieties of three of the six minerals (noted parenthetically above) to distinguish them from their massive forms, such nomenclature has not been developed for anthophyllite, tremolite, or actinolite. Therefore, when discussing these latter three minerals, it is important to specify whether a massive habit of the mineral or the fibrous (asbestiform) habit is intended.

3.2 The Health Effects of Asbestos

When disturbed by natural forces or human activities, asbestos can release microscopic fibers and more complex structures (e.g. bundles and clusters)[6] into the air and many of these structures are respirable. It is generally accepted that inhalation of such asbestos structures can lead to a range of adverse health-effects including, primarily: asbestosis, lung cancer, and mesothelioma (see, for example, Berman and Crump 2001). Asbestosis, a chronic, degenerative lung disease, has been documented among asbestos workers from a wide variety of industries. However, the disease is expected to be associated only with the higher levels of exposure commonly found in workplace settings and does not typically result from environmental asbestos exposure.

---

[6] For concise definitions of respirable asbestos structures, see ISO (1995).

The type of lung cancers that have been attributed to asbestos exposure are similar to those attributed to smoking. Further, simultaneous exposure to asbestos and cigarette smoke tends to have a multiplicative effect on the risk of developing lung cancer (Berman and Crump 2001).

Mesothelioma is a rare cancer of the membranes that line the pleural cavity (which surrounds the heart and lungs) and the peritoneal cavity (i.e. the gut). Although there is some evidence of a low background incidence of spontaneous mesotheliomas in the general population, this cancer has been associated almost exclusively with exposure to fibrous substances (HEI-AR 1991). In most cases, this means exposure to asbestos. In rare cases, however, exposure to other fibrous substances has also been linked to the induction of mesothelioma. For example, erionite (a fibrous zeolite mineral that occurs in some volcanic tuffs) has been established as the causative agent for the high rate of mesothelioma observed in some villages in Turkey (Baris 1987).

Gastrointestinal cancers and cancers of other organs (e.g. larynx, kidney, and ovaries) have also been linked with asbestos exposure in some studies. However, such associations are not as compelling as those for the primary health effects listed above and the potential risks from asbestos exposure associated with these other cancers are much lower (see, for example, Berman and Crump 2001). Consequently, by addressing the more substantial asbestos-related risks associated with lung cancer and mesothelioma, the much more moderate risks potentially associated with cancers at other sites are also addressed by default. Therefore, the risks addressed in this document are focused on lung cancer and mesothelioma.

3.3 Fibers versus Cleavage Fragments

When the massive habits of the asbestos-related minerals are crushed, elongated particles (cleavage fragments) are generated that can resemble fibers (or other asbestos structures). However, the properties of true asbestos structures differ from those of cleavage fragments. For example, true asbestos fibers tend to exhibit high tensile strength, general chemical resistance, and flexibility. Moreover, the chemical bonds on the surfaces of these structures tend to be fully satisfied (see, for example, Berman and Crump 2001). In contrast, cleavage fragments tend to be rigid and are relatively prone to chemical attack. The latter is because the chemical bonds on the surfaces of these structures tend to be incompletely satisfied.

Because the properties of cleavage fragments differ from true asbestos fibers, it is not clear to what extent such fragments contribute to the adverse health effects commonly associated with asbestos (Berman and Crump 2001). Epidemiology studies of environments in which exposure was believed to be exclusively to cleavage fragments have tended to be negative. However, as a group, cleavage fragments tend to be shorter and thicker than true asbestos fibers and studies that definitively separate

effects of dimensions from effects of crystalline habit appear to be lacking. Thus, It is not clear whether the distinction between the crystalline habits of true fibers and cleavage fragments precisely map distinctions in health effects so that questions concerning the biological activity of cleavage fragments have not been entirely resolved.

Questions concerning the health effects of cleavage fragments are further confounded by difficulties in distinguishing between such fragments and true fibers during analysis of isolated, individual structures such as those observed in air samples. For example, when asbestos is determined based on the traditional (dimensional) definition used for asbestos fibers (see, for example, NIOSH 1984), large numbers of cleavage fragments are potentially counted as fibers and, as indicated above, this does not appear appropriate for assessing risk (see, for example, OSHA 1992 and Berman and Crump 2001). Consequently, cleavage fragments were traditionally excluded from regulation (OSHA 1992). Unfortunately, procedures proposed for distinguishing fibers from cleavage fragments (when observed as isolated, individual structures) are controversial and have not been codified. Thus, no formal procedure has been established for determining whether fibrous structures of unknown origin or structures from mixed environments should be counted or excluded when addressing health effects.

In contrast, there is sufficient evidence available to define a limited range of structure dimensions that represent the set of asbestos structures that contribute to biological activity (see, for example, Berman and Crump 2001). Coincidentally, the limits of this range of structures is sufficiently narrow to exclude the vast majority of cleavage fragments that tend to be produced when the massive habits of asbestos minerals are crushed. Given the current limits to knowledge concerning the health distinctions between cleavage fragments and true asbestos fibers and the historical difficulty in distinguishing among such structures during analysis, prudence dictates that we continue to include as biologically active the limited number of cleavage fragments that nonetheless exhibit sufficiently extreme dimensions to fall within the definition of biologically active structures (as defined in Berman and Crump 2001).

Incorporating an exposure index[7] that excludes most cleavage fragments is one of the features that distinguishes the new protocol (Berman and Crump) from the traditional approach used to assess asbestos-related risks (IRIS 1988), which relies on the traditional definition of a fiber (as described above). The exposure index incorporated into the new protocol has come to be termed, “protocol structures.”

Protocol structures are defined as fibers or bundles that are observed either as isolated structures or as components of more complex clusters or matrices, that are longer than

---

[7] An exposure index is a specified range of structure sizes and shapes that are to be counted during an analysis to determine structure concentrations.

5 µm and that are thinner than 0.5 µm. The structures that are longer than 10 µm must also be distinguished from those between 5 and 10 µm in length because they are to be weighted more heavily than the shorter structures when assessing risk (Section 3.5).

3.4 Terminology for Describing Fibrous Structures

To facilitate discussion of issues associated with distinctions among various types of fibrous structures, the following terminology was developed and is used consistently throughout this document:

Asbestos structures (or true asbestos structures) are fibers or bundles or the fibrous components of clusters or matrices as defined in ISO Method 10315 (1995) that are also "asbestiform" meaning that they exhibit (most of) the properties commonly associated with asbestos (i.e. high tensile strength, resistance to chemical attack, and flexibility). Typically, the dimensions of an asbestiform fiber are determined by its growth, which differs from the manner in which the dimensions of cleavage fragments are determined. Because cleavage fragments are not asbestiform, they are excluded from this definition.

Cleavage fragments are elongated structures that are formed by the cleavage of the massive or acicular habits of an asbestos-related mineral.

Fibrous structures are fibers, bundles, clusters, or matrices as defined in ISO Method 10315 (1995), whether asbestiform or not. Thus, fibrous structures may include cleavage fragments as well as true asbestos structures.

Fibrous, biologically active structures are defined *in this document* as any structure satisfying the definitions of either protocol structures or 7402 structures.[8]

Phase Contrast Microscopy Equivalent (PCME) structures (in this study) are structures mimicking the appearance and satisfying the dimensional requirements of structures traditionally counted by phase contrast microscopy (PCM), except that they are actually characterized by transmission electron microscopy (TEM). Such structures must also be composed of an asbestos-related mineral.

[8] In contrast, 7402 structures are *not* included in the definition of biologically active structures described in the new protocol (Berman and Crump 2001).

Protocol structures are structures (including true asbestos fibers, true asbestos bundles, and cleavage fragments) that satisfy the dimensional constraints indicated in Section 3.3 and that are composed of an asbestos-related mineral.

7402 structures are structures (including true asbestos fibers, true asbestos bundles, and cleavage fragments) that satisfy the requirements for PCME structures (as defined in NIOSH Method 7402, 1989) and that are composed of an asbestos-related mineral.

3.5 Procedures for Measurement and Risk Assessment

By consensus of the Expert Group (Expert Panel-Commissioned by NJDEP/EPA 2000), it was recommended that asbestos risks be evaluated for Southdown using the procedures described in the protocol discussed above (Berman and Crump 2001).

Thus, risks should be evaluated by importing measured or estimated asbestos exposure concentrations into the dose-response models presented in the protocol for lung cancer and mesothelioma, respectively, along with the appropriate dose-response factors, which are matched for both disease end point and asbestos mineral type.[9] Moreover, measured or estimated exposure concentrations used to assess risk must be specifically matched to the same exposure index to which the models and dose-response factors of the protocol have been normalized. Thus, measured or estimated exposure concentrations must represent concentrations of protocol structures.

As previously indicated, protocol structures are all asbestos structures (separately enumerated for each mineral type) that are longer than 5 µm and thinner than 0.5 µm. The structures that are longer than 10 µm must also be distinguished from those between 5 and 10 µm in length because they are to be weighted more heavily than the shorter structures when assessing risk. It was further agreed that protocol structures are to be identified and characterized during determination of asbestos concentrations under this protocol using the counting rules defined in the ISO Method (ISO 1995).

Although the consensus of the expert panel was to evaluate risks at Southdown based on the procedures defined in Berman and Crump (2001), it was further decided that asbestos concentrations would also be measured and reported using the traditional definition for fibers but determined based on analysis using TEM (i.e. 7402 structures) and that risks would also be estimated based on these measurements using the traditional approach, which is to multiply estimated exposure concentrations by the unit risk factor for asbestos defined in IRIS (1988). In addition, a procedure developed by

---

[9] Alternatively, appropriately defined exposure estimates can be combined with appropriately normalized factors presented in Table 8-1 of the protocol to estimate risk.

RJ Lee[10] (No Date) would be employed to distinguish true asbestos fibers from cleavage fragments exhibiting similar mineralogy so that risks could be estimated with or without restricting exposure concentrations to true asbestos structures. The RJ Lee procedure is incorporated as Appendix A.

4 CORE SAMPLE COLLECTION, PREPARATION, AND ANALYSIS

4.1 Core Sample Collection

A total of 15 samples representing composites of core segments from each of five archived drill cores (a sixth drill core was found to be unusable) were acquired for analysis. The cores were originally collected in 1997 by Southdown Inc. (as described by Volkert 1999). Volkert also provides a description of the location in the Quarry from which each of the five usable cores were drilled. These locations are spatially dispersed over the surface of the commercially viable marble in the quarry.

Each (core composite) sample is designed to represent a specific, 10-ft depth interval in Quarry material and the set of 15 such samples covers the entire (approximately 150 ft) thickness of the marble body from its surface (at the time that the cores were collected) to the bottom of the marble.

4.2 Core Sample Preparation

To derive representative composites of fixed depth intervals, 1 ft core samples were selected from core segments representing the first and fifth foot depth of each 10 ft interval from each of the five useable, archived drill cores. Selected segments were each split longitudinally and one split from each of the 10 segments representing each 10 ft interval were composited (i.e. crushed, combined, homogenized, and split). Evaluation of the integrity and consistency of the core samples was performed by the NJDEP's NJ Geologic Survey which also conducted the splitting of the core segments. Crushing, combining, homogenizing, and splitting were performed at EMS Laboratories.

The crushing of each segment was accomplished using a jaw crusher that was set so that all crushed fragments would pass through a 3/8th's in (1 cm) screen. This was done to satisfy the preparation requirements of the method employed to perform the analysis (Berman and Kolk 2000). Procedures employed for homogenization and splitting are defined in Chapter 8 of Berman and Kolk (1997).

[10] RJ Lee is one of two laboratories that provided analytical services for this study.

4.3 Core Sample Analysis

Cores were analyzed using the Modified Elutriator Method (Berman and Kolk 2000), which is a modification of the Superfund Method (Berman and Kolk 1997). Briefly, the method involves placing an approximately 60 g (weighed) sample in a tumbler (one-inch square cross section), passing constant humidity air over the sample while tumbling (to pick up entrainable dust), separating out the respirable fraction of dust in a vertical elutriator, and depositing the resulting dust on a pre-weighed polycarbonate filter, which is re-weighed (to determine the quantity of dust deposited) and prepared (using a direct transfer procedure) for analysis by TEM for the determination of asbestos. Results are reported as the number of structures per microgram of respirable dust ($s/\mu g_{PM10}$).

Measurements derived using the Modified Elutriator Method offer two unique advantages over asbestos measurements derived using other bulk methods. First, in contrast to measurements derived using other analytical methods, measurements derived using the Modified Elutriator Method have been shown to represent an inherent property of the sample matrix (see Berman and Kolk 2000). Second, it has also been shown that such measurements can be combined with published dust emission and dispersion models to predict airborne concentrations of asbestos generated by disturbance of soils or other bulk materials containing asbestos and that such predictions are sufficiently accurate to support risk assessment (Berman 2000).

In this study, measurements derived using the Modified Elutriator Method are combined with modeled estimates of respirable dust concentrations at defined locations of interest that are attributable to emissions from operations at the quarry (BAQE 2001)

4.4 Core Analytical Results

Results from core composite analysis are presented in Table 1. As previously indicated (Section 3.5), counts and concentrations for asbestos in these samples are reported using each of two separate exposure indices: protocol structures and 7402 (PCME) structures.

In Table 1, the first column indicates the specific (10 ft) depth interval represented by the composite analyzed. In this column, Depth Interval 1 represents the shallowest depths sampled and Interval 15 represents the deepest. Thus, Depth Interval 1 represents material that has recently been (or is currently being) quarried.

The second column indicates the sample identification number assigned by EMS.[11] The third column indicates the mass of respirable dust (PM_{10}) deposited on the

[11] EMS is the second of two laboratories that provided analytical services for this study.

analytical filter during sample preparation using the elutriator. The fourth and fifth columns indicate, respectively, the size of the grid openings and the number of grid openings counted on the set of grid specimens that were prepared from each analytical filter for TEM analysis.

Columns 6 and 7 indicate the numbers of protocol structures and 7402 structures (respectively) observed on each set of specimen grids analyzed by TEM. Columns 8 and 9 indicate the corresponding concentrations of protocol structures and 7402 structures (respectively) estimated from the structure counts (Columns 6 and 7) for the depth interval indicated. Concentrations are reported as the number of structures per microgram of respirable dust.

The sensitivity for each analysis is presented in Column 10. Analytical sensitivity is determined for each sample analysis per the following equation:

$$AS = \frac{N_s * A_{filter}}{A_{go} * N_{go} M_{dust}} \qquad \text{(Equation 1)}$$

where:

- AS is the analytical sensitivity ($s/\mu g_{PM10}$), which is defined as the concentration equivalent to observation of a single structure;
- N_s is the number of asbestos structures (fixed at 1 for AS);
- A_{filter} is the effective surface area of the analytical filter (mm^2);
- A_{go} is the area of a grid opening on the sample specimen grid (mm^2);
- N_{go} is the number of grid openings examined during analysis (dimensionless); and
- M_{dust} is the mass of respirable dust (PM_{10}) deposited on the surface of the analytical filter (µg).

Columns 11 through 14 of Table 1 indicate, respectively: the total number of protocol structures observed during each analysis, the number of these that are longer than 10 µm, the number of total protocol structures that are also classified as true asbestos fibers or bundles (using the scheme described in Appendix A), and the number of long protocol structures that are classified as true asbestos. Note that the percentages of protocol structures that are long, that are classified as true asbestos, or that are both long and true asbestos are indicated at the bottom of each respective column. Thus, for example, 40% of the protocol structures observed are longer than 10 µm. It also appears that 33% of the protocol structures observed can be classified as true asbestos (i.e. they are not cleavage fragments).

Similarly, Columns 15 through 18 indicate, respectively, the total number of 7402 structures, the number of such structures longer than 10 µm, and the number of total 7402 structures that are also classified as true asbestos.

Note that results of blank analyses are also presented in the lower left quadrant of Table 1. There were no fibrous structures detected on any of the blanks analyzed during this project.

Several implications of the data derived from core composite analysis are readily apparent in Table 1. First, it is clear that concentrations of fibrous structures varies substantially as a function of depth interval. It appears, for example, that concentrations generally increase with depth from the shallowest (first) interval to Depth Interval 6 (in which concentrations up to 47 s/µg are observed). The only exception to this trend is Depth Interval 5 (which exhibits only low concentrations).

Concentrations of fibrous structures also appear to decrease substantially at depths greater than Interval 6, as only a few structures are observed during analysis of composites representing any of the depth intervals deeper than Interval 6. In fact, for intervals deeper than Depth Interval 10, protocol structures and 7402 structures are encountered only rarely.

Note, as described later (Section 5.2, Table 4), a formal test of consistency across depth intervals indicates that at least some of the differences in structure concentrations observed across these intervals are statistically significant.

It is also apparent that the various size categories of structures (i.e. protocol structures and 7402 structures) are largely co-located. The relative numbers of these structures appear to be highly correlated as a function of depth.

The shaded areas in Table 1 indicate multiple, related replicate or duplicate analyses that were performed on composites of specific depth intervals as part of a comprehensive Quality Control (QC) program. A description of this program (along with the results obtained from the program) are presented in the following chapter.

5 DATA QUALITY

Design objectives for the part of the Southdown study involving analysis of core samples were defined in the Quality Assurance Project Plan (EOHSI 2001) for the project. To assure that the quality of data derived from the analysis of core samples from the Southdown Quarry would satisfy the defined requirements, a range of QC analyses were performed. These include:

- duplicates (paired sets of specimen grids prepared, respectively, from filters collected during separate elutriator runs of duplicate splits of the same sample);
- T-replicates (paired sets of specimen grids prepared, respectively, from filters collected at different times during the same elutriator run on a single sample);

- replicates (repeated analyses of the same set of specimen grids either at different times by the same analyst or by different analysts from the same or different laboratories);

- lot blanks (a set of specimen grids prepared from a filter from each lot of filters used for the analyses). Two lot blanks were analyzed for each lot of filters employed; and

- sand blanks (a set of specimen grids prepared from an elutriator run of a sample of washed play sand that has been shown to be asbestos-free).

The numbers of each type of QC sample included in the overall QC program to track the performance of core composite analysis are summarized in Table 2.

Results of the evaluation of QC samples are described separately in the following sections for blanks and for replicates and duplicates.

5.1 Blanks

Because no fibers were detected in any of the filter lot blanks or any of the sand blanks that were analyzed in support of this project, it appears that cross-contamination or contamination from an outside source can be dismissed as concerns. Thus, such considerations are not further addressed.

5.2 Replicates and Duplicates

Results from analyses of replicates and duplicates are summarized in Table 3. In Table 3, Columns 1 and 2 indicate, respectively, whether samples are replicates, T-replicates, or duplicates. The third column indicates the date that each sample was analyzed. Column 4 indicates the depth interval from which the sample was derived. Column 5 indicates the (uncoded) Sample Number (assigned by EMS). Column 6 presents the number of grid openings scanned during analysis of the sample. Columns 7, 8, and 9 indicate, respectively, the number of total structures, the number of protocol structures, and the number of 7402 structures observed on each sample. Column 10 indicates the laboratory that performed the analysis. Columns 11 and 12 indicate, respectively, the mass of dust deposited on the analytical filter from each sample and the analytical sensitivity achieved during analysis.

In the last column of Table 3 a unique identifier is assigned to each analysis reported in the table. The identifier is coded as “#XX#x” in which the first number is the depth interval from which the sample was collected, the first (upper case) letter represents a specific duplicate split of the sample analyzed (either A or B), the second (upper case)

letter represents the laboratory ("R" for RJ Lee and "E" for EMS), the second number indicates the specific, unique analysis performed for that depth interval, and the last (lower case) letter indicates the specific set of grid specimens analyzed. Unique sets of specimen grids were prepared, respectively, for each split of a duplicate split and/or for each T-replicate of paired T-replicates.

In the manner summarized in Table 3, samples with the same sample number that are analyzed on different dates by RJ Lee represent internal "replicate" analyses that are performed as part of their regular, internal QC program. These are re-counts performed on the same set of specimen grids. Analyses labeled in Column 2 as "replicates" for samples with different sample numbers (Column 5) but obtained from the same depth interval (Column 4) represent blind replicate analyses performed on sets of specimen grids derived from sample filters collected at different times during the same elutriator run of a single core sample. Analyses labeled in Column 1 as "duplicates" are blind analyses performed on different sets of specimen grids derived, respectively, from sample filters collected from different elutriator runs of homogenized splits of the same core sample.

It should be noted that small discrepancies (on the order of one or two counts) between results on the raw data sheets provided by RJ Lee and their summary sheets have been corrected so that they did not affect the evaluation of QC data (or the risk assessment presented in Chapter 6). This is because the data used for data evaluation were derived exclusively from the raw count sheets.

With limited exceptions (associated with one sample), results presented in Table 3 suggest generally good agreement across both duplicates and replicates. However, the replicate analyses for Sample 210 appear to differ from one another (and from other duplicates or replicates of this sample) to a much greater degree than other replicates or duplicates presented in the table. These general observations were subjected to formal statistical analysis and results are presented in a series of additional tables.

Note, because the analytical sensitivities for the analyses reported in Table 3 are comparable (varying by no more than 5%), counts indicated on this table can be considered to be directly comparable across analyses. No adjustments are required.

Chi square analyses of replicate and duplicates

Table 4 presents results of a series of chi-square analyses (Lowry 2002) in which the numbers of either protocol structures or 7402 structures observed across a defined set of related duplicates and replicates are evaluated to determine whether such results are mutually consistent. If a particular group of analyses fails the chi-square test in this table, this implies that at least one of the analyses in the group is statistically significantly different from the others in that group.

In Table 4, the first column indicates the number of degrees of freedom for the test (which for these cases is simply one less than the number of separate analyses included in the group being tested). The second column indicates the critical value for the chi-square statistic associated with the stated number of degrees of freedom (at a 0.05 level of significance). The third and fourth columns provide calculated values for the chi-square test statistic for each indicated group of analyses, based either on protocol structure counts or 7402 structure counts, respectively. The fifth and sixth columns of the table indicate the results of comparing the test statistics reported in Columns 3 and 4, respectively, with the critical value for the test (provided in Column 2). If a particular group of analyses fails the chi-square test (based either on counts of protocol structures or 7402 structures) such a result is indicated in Columns 5 or 6 as "different." Otherwise, the conclusion is indicated as "similar." The last column of Table 4 describes the types of sample analyses included in each of the groups evaluated.

Results presented in Table 4 indicate, among other things, that concentrations of protocol structures or 7402 structures observed within the different depth intervals of the quarry are significantly different. Thus, the observation from Table1 (Section 4.4) that the concentrations of fibrous tremolite structures (either protocol structures or 7402 structures) vary substantially across depth intervals is confirmed by the result presented in the first row of Table 4. At least one (and probably several) of the observed differences across depth intervals are statistically significant.

Regarding QC analyses specifically, results in Table 4 also indicate that the four replicate and duplicate analyses representing Depth Interval 4 are mutually consistent and this is true whether counts of protocol structures or 7402 structures are considered. A similar result is obtained for the five replicate and duplicate analyses representing Depth Interval 9.

In contrast, the five analytical results representing Depth Interval 6 are not mutually consistent and this is true whether counts of protocol structures or counts of 7402 structures are considered. Therefore, at least one of the analyses reported for this depth interval is significantly different from the others.

Comparison of the structure counts reported in Table 3 among analyses representing Depth Interval 6 clearly indicate that Analysis No. 6AR3b is anomalous. Only one protocol structure is reported for this analysis when the smallest number observed during the analysis of any other replicate or duplicate is 11. Moreover, the ratio of protocol structures to 7402 structures reported for this analysis is substantially smaller than the ratio observed in any of the four other duplicate or replicate analyses in this group. This is true despite the generally good correlation observed between counts of protocol structures and 7402 structures across the data set as a whole.

Given the above-described differences, the chi square analysis was repeated for Depth Interval 6 with the results from Analysis No. 6AR3b omitted. However, as the results in Table 4 indicate, omitting this analysis is not sufficient to remove the source of the lack of agreement among the remaining analyses representing Depth Interval 6. Therefore, the results of Analysis No. 6AE4b were also omitted from the chi square evaluation. 6AE4b is a replicate analysis of 6AR3b performed on the same set of grid specimens and counts from this analysis also appear anomalously low relative to other replicates or duplicates reported for Depth Interval 6.

When both replicate analyses of Sample 210 are omitted from the group of analyses representing Depth Interval 6, the chi-square statistics calculated both for counts of protocol structures and for 7402 structures decrease dramatically (Table 4), which indicates improved agreement among the remaining samples. In fact, when considering counts of 7402 structures, the remaining analyses of samples from Depth Interval 6 can no longer be considered inconsistent. Moreover, while evaluation of the protocol structure counts among these remaining samples still suggests a significant lack of consistency at the 0.05 level of significance, they are consistent at the 0.01 level of significance (critical value = 9.2103).

The above combination of results suggests that one or more problems appear to have arisen in association with the preparation or analysis of the set of grid specimens specifically representing Sample No. 210. Both analyses (Nos. 6AR3b and 6AE4b) of these specimen grids produced anomalously low results. At the same time, that the remaining replicate and duplicate analyses of samples representing Depth Interval 6 show at least fair agreement, suggests that this is likely an isolated incident that should not adversely affect the overall evaluation of the data from core composite analyses. Nevertheless, potential sources of error in these analyses were further explored to determine the degree with which they might suggest broader problems.

Pair-wise comparisons of replicate and duplicate results

Table 5 presents pair-wise comparisons between replicate or duplicate analyses. Paired analyses evaluated here are subsets of the groups of replicates and duplicates reported in Table 3 and evaluated (as entire groups) in Table 4. The pair-wise comparisons are evaluated to better understand the sources of significant differences observed among some groups of replicate and duplicate analyses.

The first column of Table 5 indicates the depth interval represented by each pair of analyses. The second and third columns indicate the unique analysis identifiers for each analysis of the specific pair of analyses being compared.

Columns 4, 5, and 6 of Table 5 provide the calculated value of the test statistic comparing counts of total structures, protocol structures, or 7402 structures

(respectively) across the two analyses being compared. The test statistic in this case is determined as:

$$(a - b)/(a + b)^{0.5} \qquad \text{(Equation 2)}$$

where a and b are the counts of the number of structures observed during the first and second analysis of the pair, respectively.

The critical value for the test statistic is based on the fact that a Poisson Distribution can be approximated as a normal distribution with (in this case) a mean of zero and a standard deviation of 1. The critical value (z-value for the normal distribution) for such a distribution (at the 0.05 level of significance, two-tailed) is 1.96. Note that this procedure is equivalent to comparing the results of paired measurements using a chi square analysis with the critical value derived from a chi-square distribution with one degree of freedom (see, for example, Box et al. 1978). The difference is that the equation used for calculating the test statistic and the critical value are the square roots of those used in a chi square test.

Columns 7, 8, and 9 of Table 5 indicate whether the null hypothesis (that the results of the two analyses being compared are consistent) should be rejected. If the test statistic is smaller than the critical value, which indicates that one cannot reject the null for a particular pair, than the two analyses are concluded to be similar. If the critical value is exceeded, the null hypothesis is rejected and the two analyses are concluded to be different.

The last column of Table 5 indicates that types of analyses being compared. These may include:

- within or between laboratory replicates;
- within or between laboratory T-replicates;
- analyses of duplicate splits analyzed by the same laboratory; or
- analyses of duplicate splits analyzed by different laboratories.

Results presented in Table 5 indicate that, consistent with the results presented in Table 4, all analyses representative of Depth Intervals 4 and 9 are mutually consistent. Also, consistent with the results in Table 4 is the observation that at least some of the pair-wise comparisons of analyses representing Depth Interval 6 are significantly different.

Several inferences concerning the analyses representing Depth Interval 6 can be drawn from the comparisons presented in Table 5. Note also that the individual counts derived during each of the analyses discussed here are presented in Table 3. These indicate, for example, that the between-replicate analyses (6AE1a and 6AR2a) of the

first set of specimen grids from Sample 207 are mutually consistent. Either of these analyses also appear to be generally consistent with the analysis of the duplicate sample from this set (6BR5c), although agreement with this third analysis is not quite as good as the agreement between the two replicate samples.

For example, comparison between 6AR2a and 6BR5c shows consistency whether the comparison is based on counts of protocol structures or counts of 7402 structures. Moreover, although counts of total structures differ among these two samples at the 0.05 level of significance (Table 5), they are consistent at the 0.01 level of significance (critical value = 2.58). Consistency between 6AE1a and 6BR5c is marginal.[12] While counts of 7402 structures among these two samples are consistent, counts of protocol structures are different, even at the 0.01 level of significance (although the critical value is only slightly exceeded in this case).

In contrast, much larger variation is observed between the duplicate sample (6BR5c) and either of the replicate analyses conducted on the set of specimen grids designated as Sample 210 (Analyses 6AR3b and 6AE4b). These differences are highly significant whether the comparisons are based on total structure counts, protocol structure counts, or counts of 7402 structures. Further, comparisons between either replicate analysis of Sample 210 and either replicate analysis of Sample 207 also show that they are significantly different, at least for comparisons based on total structures or protocol structures. However, comparisons based on counts of 7402 structures in this case do not show differences.

These observations further confirm a potential problem either with the preparation or analysis of the grid specimens designated as Sample 210 and they provide some clues as to the source of the problem. For example, that analyses of Sample 210 by both laboratories are inconsistent with the other QC analyses suggest that the problem is more likely associated with preparation than analysis (serious random errors by two, independent laboratories are unlikely to occur on the same sample). Therefore, the problem may relate to such things as lack of uniformity of the original deposit on the filter, whether the mass of the original deposit on the filter was accurately recorded, and/or whether damage or other difficulties resulted in losses during direct transfer from the filter to the specimen grids representing this sample. These and similar considerations are explored further below.

---

[12] It should be noted that differences between analysis 6AE1a and any other analysis to which it is compared may be due at least partially to the excessive, prior handling of the specific set of grids specimens on which this analysis was conducted as these specimens were (blind) shipped back and forth between laboratories. Such handling frequently results in breakage of the carbon coat, particularly on grid openings containing structures, which are consequently lost. Thus, counts on such filters become lower and more variable with time. It is therefore not surprising that this particular analysis exhibits lower counts than any previous analysis of these grid specimens. Of course, the magnitude of this effect cannot be quantified. The effect can only be noted as a mitigating factor.

Tests of the uniformity of filter deposits

To explore the possibility that deposits on analytical filters prepared using the Modified Elutriator Method may not be uniform, chi-square analyses were conducted to evaluate the consistency in the numbers of structures observed across individual grid specimens derived from the filters prepared for core analysis during this study.

Counts of the numbers of structures observed on individual grid specimens were obtained from the raw count sheets provided by each laboratory. The results of the chi-square analysis of these counts are presented in Table 6.

In Table 6, the first column indicates the identifier for each analysis. The depth interval represented by each respective analysis is presented in the second column. The third column of the table indicates the sample number from which each analysis derives. The fourth column indicates the number of degrees of freedom for each evaluation and the fifth column presents the critical value (corresponding to the 0.05 level of significance) for a chi-square distribution for the indicated number of degrees of freedom.

Note that, although five grid specimens were prepared from each sample filter collected over the elutriator (which corresponds to four degrees of freedom in the analysis), for some unknown reason, one of the laboratories did not always spread their analysis across all five grid specimens. Therefore, the number of degrees of freedom is not the same for all of the analyses presented in Table 6. For each analysis, the number of degrees of freedom is one less than the number of grid specimens included in the analysis.

The sixth, seventh, and eighth columns of Table 6 present the chi-square statistic calculated for each set of specimen grids representing each analysis based on counts of total structures, protocol structures, or 7402 structures, respectively. The last three columns of the table indicate the results of comparing the calculated chi square test statistic to the critical value.

As indicated in Table 6, with the exception of two tests (one based on 7402 structures for Analysis 6AE4b and one based on total structures for Analysis 9AR2b), there is no other indication that counts of structures observed among different grid specimens prepared from the same filter are significantly different Moreover, of the two exceptions, the chi-square statistic for counts of total structures for Analysis 9AR4b differs from the critical value by less than 0.1% so that it can be eliminated from further consideration.

Although the single remaining evaluation (for counts of 7402 structures among Analysis 6AE4b) in Table 6 that suggests a lack of uniformity does involve a test of the

specimen grids representing Sample 210, which is the sample suspected of being anomalous, the test statistic even for this sample is less than the critical value at the 0.01 level of significance. Therefore, not even this result indicates a lack of uniformity. Moreover, the distribution of protocol structures on this sample shows no indication of lack of consistency and there is no known mechanism by which the distribution of fibers in a restricted size range would be non-uniform while all other size ranges are uniform. In fact, the test statistic for protocol structures in this case cannot be rejected even at a 0.2 level of significance. Moreover, given that 85% of the test statistics presented in Table 6 cannot be rejected at the 0.1 level of significance, 67% cannot be rejected at the 0.2 level of significance, and that the random chance of observing a single anomaly among 27 independent statistical analyses is not small, the data in Table 6 strongly suggest that filters collected over the elutriator during this project were all adequately uniform so that this possibility can be dismissed as a general concern and as an explanation of the apparent, inconsistent results across the specific analyses representing Depth Interval 6.

Note, a second potential source of variation is due to differences in the *quality* of deposit (i.e. the relative asbestos to dust ratio) that is deposited at different times within a single elutriator run. This source of variation can be eliminated from concern, however, due to lack of any plausible mechanism for generating such a difference and lack of any evidence that such a difference has ever occurred over the course of history of use of the elutriator. In fact, elutriator runs have shown to emit material in an extremely regular and predictable manner. Emission rates from the tumbler have been shown to follow a first order decay with no measurable variation; agreement between prediction and time-dependent measurements of cumulative dust emitted from the tumbler show r^2 values of 0.9999 or better.

Other candidate sources of error

Given the results of the set of statistical analyses described above, inaccurate recording of the dust mass deposited on the filter designated as Sample 210 remains as a leading candidate to explain at least some of the problems that have been observed with this sample. Specifically, if the dust mass estimated for this filter was shown to be anomalously high and could be corrected, it would reduce the apparent discrepancy between structure counts observed among replicate analyses of grid specimens prepared from this filter and the other replicate and duplicate analyses of samples representing Depth Interval 6.

Unfortunately, there is no independent way to reconstruct or re-verify the recorded value. Moreover, inaccurate recording of the mass for this sample cannot explain the observed variation in the ratio of protocol structures to 7402 structures among the two replicate analyses of the grid specimen set from this filter. Thus, inaccurate recording

of mass would not entirely explain the inconsistencies observed between this sample and related samples.

There is no known mechanism associated with the handling, preparation, or analysis of these samples that could cause the required, extensive size-selectivity between these two analyses that would be required to generate the observed difference in the ratio of protocol structures to 7402 structures (i.e. a ratio of 2.4 versus a ratio of 0.17, which differ by a factor of 14). Thus, some other type of analytical or recording error may also have occurred involving incorrect categorization of the fibrous structures observed. This is required specifically to explain the observed counts from analysis 6AR3b. The anomalously low counts observed in analysis 6AE4b, because it exhibits a ratio of protocol structures to 7402 structures that is more in line with other replicate and duplicate analyses can potentially be explained by nothing more than an inaccurately recorded dust mass for this filter.

5.3 Conclusions QC for Core Composite Analyses

Overall the evaluation of blanks, replicates, and duplicates associated with the preparation and analysis of core composites from the Southdown Quarry indicate generally good performance. Although replicate analyses of one set of specimen grids from among a group of replicate and duplicate analyses appear to be anomalously low, the source of this problem appears to be a random reporting and/or analytical categorization error. No other problems were observed.

The two low analyses are between laboratory replicates conducted over a common set of specimen grids that are among three sets of specimen grids representing replicates, T-replicates, and a duplicate split prepared from the same material (Depth Interval 6). Multiple analyses of the other two sets of specimen grids prepared from this same material show reasonable agreement. Moreover, sources of error that could potentially explain the anomalous results were explored and those that might suggest problems with the broader data set were eliminated as concerns. Further, two other groups of replicate/duplicate analyses (on samples representing Depth Interval 4 and Depth Interval 9, respectively) show good within-group agreement with no apparent problems.

Thus, it is likely that the problem observed in association with the single sample (among the samples representing Depth Interval 6) is an isolated incident. It is unlikely to adversely affect use of the broader data set to support risk assessment. At the same time, because the source of the observed inconsistencies cannot be precisely determined (what is likely to be at least partially analyst or reporting error is difficult to document), the data need to be evaluated carefully. Thus, we attempted to interpret the data in a manner that is robust to concerns raised by the anomalous results.

6 RISK ASSESSMENT

The results of core composite analyses are recapitulated in Table 7 but presented in a manner suitable for supporting risk assessment. Unlike Table 1, results from replicate and duplicate analyses are averaged in Table 7 so that their values are not over weighted when the data are pooled.

In Table 7, Columns 1 through 10 are identical to those presented in Table 1 (except that values from blank analyses are no longer shown). Column 11 presents the reciprocal of the analytical sensitivity for each of the analyses conducted, except that the reciprocals for replicate and duplicate samples are averaged so that only a single value is presented for each unique depth interval. Columns 12 through 15 present, respectively, counts of total protocol structures, long protocol structures, protocol structures that are classified as true asbestos fibers (or bundles), and long structures that are classified as true asbestos fibers (or bundles) for each depth interval analyzed. For Columns 12 though 15 (as with Column 11), counts are averaged over replicates and duplicates so that each unique depth interval is associated with a single, "best estimate" count for each type of structure. Similarly, Columns 16 through 18 present counts of 7402 structures, long 7402 structures, and 7402 structures that are also classified as true asbestos.

It is readily apparent in Table 7, as previously indicated, that the concentrations of the fibrous structures of interest vary substantially as a function of depth. Moreover, as previously shown (Section 5.2) at least some of these differences across depth intervals are significant. It appears, for example, that the first three intervals (to a depth of 30 ft) contain similarly low but detectable concentrations of protocol structures and 7402 structures, respectively. The non-contiguous fourth and sixth depth intervals exhibit substantially higher concentrations of these structures. In the deeper intervals (i.e. Intervals 11 and higher), which begin at a depth of approximately 110 ft, protocol structures and 7402 structures are only rarely detected.

Given the above, it is expected that emissions of protocol structures and 7402 structures attributable to quarry operations may vary substantially with time as each depth interval quarried provides a changing contribution to the source concentration. However, cancer risk is a function of lifetime exposure. Therefore, because each core segment represents only approximately 10 years of quarry production, we averaged across core segment concentrations, as appropriate to derive long-term average exposure estimates.

The data presented in Table 7 were used as described below to assess risks attributable to emissions of fibrous, biologically active structures from the Quarry that might be experienced by residents living in the vicinity. As indicated in Section 3.5, risks are estimated using each of two approaches: one based on protocol structure

counts and one based on 7402 structures counts. Results from each are described below and these results are evaluated and compared to support conclusions and recommendations.

6.1 Approach for Evaluating Risks Attributable to Emissions of Biologically Active Structures from the Southdown Quarry

The general approach adopted for evaluating risks in this report was to:

1. model advective and dispersive transport of respirable particulate matter (PM_{10}) that is emitted by quarry operations to locations where residents might become exposed;

2. determine the ratio of protocol structures (and 7402 structures) to PM_{10} in the bulk phase;

3. apply the measured ratios to convert modeled exposure concentrations of PM_{10} to estimated exposure concentrations of protocol structures (and 7402 structures); and

4. apply the dose-response factors recommended in Berman and Crump (2001) for protocol structures (or the IRIS unit risk factor for 7402 structures) to estimate risk from the corresponding exposure concentrations.

The manner in which each of these steps was accomplished is described briefly below.

6.1.1 Modeling emissions and transport of respirable particulate matter

For the Southdown Quarry, concentrations of PM_{10} attributable to the total, combined emissions from the quarry were modeled by a team at the NJDEP Bureau of Air Quality Modeling (BAQE 2001). The modeling was performed primarily to evaluate compliance with nuisance dust standards as part of a larger investigation of compliance issues related to the quarry (J. Held, NJDEP, private communication).

As part of this modeling effort, maximum annual concentrations of PM_{10} were estimated for the area immediately surrounding the Southdown Quarry. Maximum annual concentrations are the largest of the mean annual concentrations estimated among the years of meteorological data employed in the modeling effort. Therefore, these represent conservative (in a health protective sense) estimates of exposure concentrations that address variation in meteorology. The isopleth map depicting the maximum annual concentrations are reproduced in this report in Figure 1. The map depicted in Figure 1 represents a model run incorporating only sources of marble-

related emissions from the quarry. Fibrous, biologically active structures are unlikely to be associated with emissions of non-marble related dust.

The annual average depicted in Figure 1 is for the meteorological data representing 1990, which produced the highest mean annual average concentrations among all of the years modeled (1990 - 1992).

Figure 1 is a map of the area surrounding the Southdown Quarry. The boundaries of the Southdown Quarry are depicted in black along with the major roads located within the quarry boundaries. The closed loops superimposed on this figure represent lines of constant concentration (isopleths) for maximum annual PM_{10} concentrations (in $\mu g/m^3$).

As can be seen in Figure 1, the greatest maximum annual concentration observed at any location is 45 $\mu g/m^3$. The greatest (maximum annual) concentration at the northern boundary to the quarry is 15 $\mu g/m^3$. Similarly, the greatest (maximum annual) concentration at the southern boundary to the quarry is approximately 4 $\mu g/m^3$. Also, because the 1 $\mu g/m^3$ isopleth is closer to the quarry than the nearest residences, the maximum mean annual exposure concentrations potentially experienced by neighboring residents would be less than 1 $\mu g/m^3$. These values are employed in the following risk assessment to represent, respectively, the most extreme worst case value for any hypothetical receptor, the worst case estimate for offsite residents, a most extreme worst case estimate for the offsite residents living to the south of the quarry (where the closest residents actually reside), and a reasonable upper bound estimate of the concentrations in the immediate vicinity of the closest actual residences to the quarry.

Importantly, even the lowest of the PM_{10} concentrations described above should be considered to be highly conservative (in a health protective sense) for two reasons. First, emission estimates used as inputs for modeling are based on maximum allowable permit limits and conservative estimates of any un-permitted emissions It is therefore expected that any actual emissions would be substantially lower. Second, these estimates were modeled using the single year of historical meteorological data for which the highest concentration estimates were obtained (rather than being modeled as an average over the years of available meteorological data).

As previously indicated, the concentrations of PM_{10} represented in Figure 1 are derived based on combined emissions from all of the major sources that reportedly involve handling of the marble at the Southdown quarry, which is appropriate for the risk calculations performed below. Moreover, the duration and frequency of each operation (over the course of the year modeled) was adjusted to represent the best available estimates for that operation. Therefore, when estimating risk, no adjustments were incorporated for duration and frequency of exposure because it is assumed

(conservatively) that residents would be home over the entire period that any of the operations at the quarry might be performed.

6.1.2 Determining the ratio of protocol structures and 7402 structures to respirable dust

As previously indicated (Chapter 4), the concentrations of protocol structures and 7402 structures in the bulk phase were determined by crushing and compositing core samples and analyzing them per the Modified Elutriator Method (Berman and Kolk 2000). Also per the method, results from these analyses are reported as the ratio of each size range of structures to the mass of respirable dust (PM_{10}) simultaneously liberated from the sample. These are precisely the ratios required for estimating risk in this approach.

Measured concentrations expressed in terms of the desired ratios (in structures/µg dust) for protocol structures and 7402 structures, respectively, are presented in Columns 8 and 9 of Table 7. Similar concentration estimates (expressed in terms of the desired ratio) can also be derived from counts of any of the structure types presented in Columns 12 through 18 of the table by simply multiplying each count by its corresponding analytical sensitivity (Column 10). The mean concentrations from the pooled data can also be determined by multiplying any of the total counts (presented at the bottom of Columns 12 through 18) by the analytical sensitivity derived for the pooled data (presented at the bottom of Column 11).

As previously indicated (Section 4.3), the Modified Elutriator Method is specifically designed to provide a determination of the concentration of structures (within a defined size range of interest) per unit of respirable dust emitted when the bulk material analyzed is disturbed by either natural forces or human activities. That measurements of this ratio in the bulk phase (derived using this method) relate to the same ratio in the air (following emissions due to any of various types of disturbance) was demonstrated in a previous study (Berman 2000). In addition, the theory behind the link between these bulk phase measurements and airborne concentrations is described in the Background section (Chapter 3) of the method document itself (Berman and Kolk 2000).

6.1.3 Estimating exposure concentrations of fibrous, biologically active structures

As indicated by a dimensional analysis, estimates of the airborne exposure concentrations of protocol structures, 7402 structures, or any other structure types reported in Table 7 are derived simply by multiplying the measured ratios of structures to dust (derived as described in Section 6.1.2) by the concentration of PM_{10} estimated

at each location of interest (as described in Section 6.1.1). Results for protocol structures are provided in Table 8.

In Table 8, the first column indicates the location from which the maximum annual average PM_{10} concentration was selected for estimating exposures to protocol structures in the corresponding row. The second column provides the corresponding value for the PM_{10} concentration at that location. Estimated exposure concentrations for protocol structures for the locations indicated are provided in the third column of the table (in s/m^3). These are derived by multiplying the mean concentrations from the pooled measurements of protocol structures in Table 7 (modified as described below) by the PM_{10} concentrations indicated in the corresponding row of Table 8. The estimated airborne exposure concentrations of weighted protocol structures presented in Column 3 of Table 8 are converted to units of s/cm^3 in the fourth column so that they can be used to estimate risk (see Section 6.1.4).

Importantly, the protocol structure concentrations indicated in Table 8 are weighted to reflect the relative contributions of short and long protocol structures to risk. It is the concentrations of weighted protocol structures that remain proportional to risk (see Berman and Crump 2001). Weighted concentrations of protocol structures are derived by substituting the number of short and long protocol structures (derived, respectively, from Columns 12 and 13 of Table 7)[13] into the following formula (as recommended in Berman and Crump 2001):

$$C_{prot} = 0.003*C_{short} + 0.997*C_{long} \qquad \text{(Equation 3)}$$

where:

C_{prot} is the weighted concentration of protocol structures appropriate for estimating risk;

C_{short} is the measured concentration of protocol structures between 5 and 10 µm in length; and

C_{long} is the measured concentration of protocol structures longer than 10 µm.

To derive concentration estimates, as previously indicated, the observed number of weighted structures indicated at the bottom of Table 7 are simply multiplied by the corresponding analytical sensitivity for the measurement (presented in Column 11).

---

[13] The number of short protocol structures observed in the various measurements is simply the number of total structures (presented in Column 12 of Table 7) minus the number of long structures (presented in Column 13).

Due to implications concerning risk (see Section 6.1.4), exposure concentrations of the subset of weighted protocol structures that are also classified as true asbestos fibers (see Table 7) are also presented in Columns 6 and 7 of Table 8.

Exposure estimates for 7402 structures are presented in Table 9. The format for Table 9 is identical to that described for Table 8, except that concentrations are presented in Columns 3, and 4 for 7402 structures (rather than protocol structures) and in Columns 6 and 7 for 7402 structures that are also classified as true asbestos fibers (rather than protocol structures). Exposure concentrations of 7402 structures are estimated in a manner similar to that described above for protocol structures, except that 7402 structures are not weighted. Thus, exposure concentrations for 7402 structures are determined simply by multiplying the mean concentration for the pooled values (presented at the bottom of Table 7) by the modeled PM_{10} concentrations in the corresponding row of Table 9.

6.1.4 Estimating risks attributable to exposure to fibrous, biologically active structures

Risks posed by emissions of fibrous, biologically active structures from the Southdown quarry are estimated from exposure concentrations in the manner indicated in Section 3.5. As previously indicated, such risks are estimated separately based both on protocol structure counts and 7402 structure counts.

Risks based on protocol structure counts

For protocol structures, risks are estimated by combining exposure estimates with the appropriate risk factor selected from the appropriate cell of Table 8-1 in Berman and Crump (2001). That table is reproduced as Table 10 in this document.

Table 10 provides estimates of risk (for lung cancer, mesothelioma, and the two combined) based on a life-table analysis incorporating the recommended EPA models for these diseases and dose-response factors that are matched to the recommended exposure index (i.e. protocol structures). This specific table is developed assuming lifetime, continuous exposure at a level of 0.0005 s (as protocol structures)/cm^3 air.

Note that the weighting of protocol structures is performed automatically in this table so that what is required to use the table are estimates of the concentration of total protocol structures and the percentage of such structures that are longer than 10 µm. The specific column of the table to be used to estimate risk is selected based on the percentage of protocol structures among the total that are long. The first column in table 10 indicates a specific receptor group for whom risk is estimated.

Risks estimated based on counts of protocol structures in this study are presented in Column 5 of Table 8. They were calculated by dividing the concentrations presented in Column 4 by 0.0005 (the reference concentration in Table 10) and multiplying the resulting quotient by the selected risk factor in Table 10. Because the mineral of interest in this case is tremolite, which is an amphibole, the risk factors presented in the bottom half of Table 10 are the relevant factors.

The specific risk factor used in this study is the most conservative factor for combined risks selected from among the indicated receptor types (i.e. the factor for female non-smokers). Because approximately 43% of observed protocol structures are long (Table 7), the risk factor listed in the bottom half of Table 10 for non-smoking females in the column representing 50% long structures is selected for this study. The corresponding value is 375. Note, however, that this value varies by less than 25% from the values for risk factors representing any of the other receptor types, so the effect of selecting a particular receptor type is small.

Due to questions concerning the distinction between true asbestos fibers and cleavage fragments, risks were also estimated for the subset of protocol structures that were also classified as true asbestos fibers (Table 7). These risk estimates are presented in Column 8 of Table 8. Comparing the corresponding results in Columns 5 and 8 of this table, it is clear that the effects of separating out true fibers among total protocol structures is small. The corresponding values vary only by about a factor of two, which is not a substantial difference for risk estimation. Moreover, given the uncertainties in the risk estimates presented, this difference is unlikely to be significant.

Risks based on 7402 structure counts

Per the procedures described in Section 3.5, risks were also estimated based on counts of 7402 structures. Results are presented in Column 5 of Table 9. Risks are estimated from 7402 structures by multiplying the concentrations presented in Column 4 by the traditional EPA unit risk factor for asbestos, which is 0.23 (IRIS 1988).

Due to questions concerning the distinction between true asbestos fibers and cleavage fragments, risks were also estimated for the subset of 7402 structures that are also classified as true asbestos fibers (Table 7). These risk estimates are presented in Column 8 of Table 9. Comparing the corresponding results in Columns 5 and 8 of this table, it is clear that the effects of separating out true fibers among total 7402 structures is moderate and substantially larger than the effect for protocol structures. The corresponding values for 7402 structures vary by more than a factor of five (almost a factor of six) while the values for protocol structures vary by only a factor of two.

Given the regulatory requrement that 7402 structure counts include only true fibers (IRIS 1988), this illustrates why it is important to specifically identify which structures

are true fibers (and exclude other structures) when assessing risk based on the traditional approach. The need for excluding such structures when assessing risks based on protocol structures is less clear since most nontrue fibers do not meet the definition of protocol structures.

Conclusions concerning risk

A brief comparison of risks derived using each of the two approaches is presented below followed by a general discussion of the risks estimated in this study.

Comparing risk estimates derived, respectively from protocol structures and from 7402 structures

Comparing risks estimated respectively based on protocol structures and 7402 structures for corresponding locations, it is apparent that risks estimated based on protocol structures are about 25 times greater.

Among the reasons for this difference is that the new approach for evaluating risks using protocol structures (Berman and Crump 2001) assigns different potencies to amphiboles and chrysotile while the traditional approach (IRIS 1988) assigns similar potencies to both. Substantial evidence supporting a difference in potency between these two general types of asbestos minerals (with amphiboles exhibiting greater potency, particularly toward mesothelioma) has been published since the traditional approach for assessing asbestos-related risks was developed. Much of this evidence is reviewed in Berman and Crump (2001). Thus, because the protocol structures observed at the Southdown quarry are tremolite and tremolite is an amphibole, the new approach assigns substantially greater potency to these structures relative to the traditional approach.

The risks estimated based on protocol structures is also greater than those estimated based on 7402 structures due to two additional, conservative factors included in the calculation of risk based on protocol structures that are not incorporated in risk estimates based on 7402 structures. First, the estimated fraction of long protocol structures (among total structures) was rounded up to select the appropriate dose-response factor from Table 10. Second, the dose-response factor selected from Table 10 is based on the receptor population for whom the effects of asbestos are greatest (i.e. non-smoking females). In contrast, risks estimates derived from 7402 structures are independent of the fraction of long structures and the unit risk factor employed to estimate these risks is “population averaged” meaning that it is adjusted for the relative numbers of smokers and the relative numbers of males and females in the general population.

Although the degree of bias introduced by the last two factors discussed above is

relatively small (combined they contribute a little less than a factor of two), they still contribute measurably to the observed difference in risk estimates. Clearly, the largest contribution to the differences in risk estimates derives from the reclassification of risk in the new protocol to assign a greater weight to exposure from amphiboles, which appears justified (as previously discussed).

General risk considerations

As previously indicated, the modeled estimates of PM_{10} concentrations used to derive risk estimates in this study are conservative (Section 6.1.1). In fact, even the lowest estimate (presented in the last row of Column 2 of Tables 8 and 9) is likely to be substantially conservative for reasons previously discussed. For this reason, PM_{10} concentrations were combined with best estimates of the mean concentrations of protocol structures (or 7402 structures) rather than upper bound estimates, so as not to introduce redundant conservatism into the calculations.

As indicated in the bottom rows of Tables 8 and 9, the level of risk potentially experienced by the nearest offsite residents is less than $1x10^{-5}$ (based on protocol structures) and $6x10^{-7}$ (based on 7402 structures). These values are entirely consistent with the low, background level of risk estimated for the same residents in the earlier study of air and dust (Lioy et al. 2002). Thus, operations at the quarry appear to pose a risk of less than one-in-one-hundred-thousand (i.e. $1x10^{-5}$) to residents in this area. Such a level of risk is well within the range of one-in-one-million (i.e. $1x10^{-6}$) to one-in-ten-thousand (i.e. $1x10^{-4}$) lifetime cancer risk within which the USEPA considers acceptability for specific sites. The same range is generally considered by the New Jersey Department of Environmental Protection (NJDEP) to be consistent with permitting of air emission sources with possible consideration of source modification.

Based on Figure 1, it also appears that risks attributable of quarry operations generally remain within the acceptable risk range of $1x10^{-4}$ to $1x10^{-6}$ up to the property boundaries. Although the maximum mean annual concentrations depicted in this figure show a small area to the north in which the projected PM_{10} concentrations exceed 10 $\mu g/m^3$.(which approximately corresponds to an asbestos-related risk of $1x10^{-4}$), this area is only 400 m long and extends no more than 50 m from the fence line. Moreover, as previously indicated, these values are substantially conservative (in a health protective sense) and, more important, there are no residents living even close to this area. Thus, since the risks estimated in this document (among other things) can be considered to represent risks projected forward in time as the marble at Southdown continues to be quarried, it is unlikely that the quarry poses unacceptable risks either to current, actual residents in the area or to any hypothetical, future residents who may move into the area.

Due to the controversy surrounding differences in the health effects of cleavage

fragments and true asbestos structures, it is instructive to examine risks specifically attributable to true asbestos. As previously indicated (see above section on protocol structures). risk estimates derived, respectively, based on total protocol structures and protocol structures classified as true asbestos differ by less than a factor of two and such differences are not likely significant. Differences between risk estimates based, respectively on total 7402 structures and 7402 structures classified as true asbestos are somewhat larger (a factor of almost six) and the regulations suggest a need to make such distinctions when risk are estimated in this manner.

The above considerations beg the question as to whether true asbestos actually exists within the marble of the quarry. Although the procedure defined by RJ Lee for distinguishing true asbestos structures from cleavage fragments (Appendix A) was employed in this study to delineate between such structures, this (and similar procedures proposed by others) is not without controversy. Thus, a small number of additional analyses were conducted by EMS in which the marble in the core samples was dissolved with acid so that the residual minerals could be concentrated. Optical microscopy of the residual material in these samples indicates that at least some of the tremolite is indeed asbestiform. Photographs taken of some of these cotton-like clusters clearly demonstrate that at least some asbestiform material is present (Figure 2).

Given the above, it appears that the marble in the quarry contains tremolite that occurs in a variety of crystalline habits and at least a small amount of this material is asbestiform. Thus, evaluation of this mixed environment was not unwarranted. Nevertheless, based on the results of both this study and the previous study of air and dust (Lioy et al. 2002) indicate that any risks to offsite residents posed by the low concentrations of asbestiform tremolite (or cleavage fragments from any other form of tremolite that is present) are less than one-in-one-hundred-thousand and well within the range generally considered acceptable by regulators. Moreover, such risk should likewise remain acceptable even as quarry operations continue into the future.

7 CONCLUSIONS AND RECOMMENDATIONS

With one exception, evaluation of the quality control data (blanks, replicates and duplicates) from this study indicate good overall performance that achieved the quality objectives stated in the Quality Assurance Project Plan for this project (EOHSI 2001). Moreover, because the one exception involves inconsistent results among replicate analyses of a single sample and the source of the inconsistencies appear to be due to an isolated recording or characterization error by an analyst, the broader data set from this study should be considered generally usable to support their intended purpose.

Evaluation of risks to neighboring residents posed by emissions of asbestos (or other fibrous, potentially biologically active structures) due to operations at the Southdown

Quarry indicate that they are likely less than one-in-one-hundred-thousand, which is well within the risk range (of 1E-4 to 1E-6) that is generally considered acceptable by regulators. Moreover, risks are projected to remain within this risk range for either existing or hypothetical future residents even as quarry operations continue into the future.

Importantly, the risks estimated in this study likewise remain acceptable whether cleavage fragments are included or excluded during determination of exposure. Further, similar conclusions are reached whether risks are estimated based on concentrations of protocol structures or concentrations of 7402 structures.

8 REFERENCES

Baris, Y.I., Simonato, L., Artvinli, M., Pooley, F., Saracci, R., Skidmore, J., Wagner, C., (1987) "Epidemiological and Environmental Evidence of the Health Effects of Exposure to Erionite Fibres: A Four-Year Study in the Cappadocian Region of Turkey." *International Journal of Cancer,* Vol. 39, pp. 10-17.

Berman, D.W. (2000) "Asbestos Measurement in Soils and Bulk Materials: Sensitivity, Precision, and Interpretation – You *Can* Have It All." in *Advances in Environmental Measurement Methods for Asbestos, ASTM STP 1342,* M.E. Beard, H.L. Rook, Eds., American Society for Testing and Materials. Pp. 70-89.

Berman, D.W. and Crump, K.S. (2001). *Technical Support Document for a Protocol to Assess Asbestos-Related Risk*. Prepared for Mark Raney, Volpe Center, U.S. Department of Transportation, 55 Broadway, Kendall Square, Cambridge, MA 02142. 2001. Under EPA Review.

Berman, D.W. and Crump, K.S. (1999a) *Methodology for Conducting Risk Assessments at Asbestos Superfund Sites. Part 1: Protocol.* Prepared for: Kent Kitchingman, U.S. Environmental Protection Agency, Region 9, 75 Hawthorne, San Francisco, California 94105. Under EPA Review.

Berman, D.W. and Crump, K.S. (1999b). *Methodology for Conducting Risk Assessments at Asbestos Superfund Sites. Part 2: Technical Background Document.* Prepared for: Kent Kitchingman, U.S. Environmental Protection Agency, Region 9, 75 Hawthorne, San Francisco, California 94105. Under EPA Review.

Berman, D.W. and Kolk, A.J. (2000). *Draft: Modified Elutriator Method for the Determination of Asbestos in Soils and Bulk Materials, Revision 1.* Submitted to the U.S. Environmental Protection Agency, Region 8. May 23.

Berman, D.W. and Kolk, A.J. (1997). *Superfund Method for the Determination of Asbestos in Soils and Bulk Materials.* Prepared for the Office of Solid Waste and Emergency Response, U.S. Environmental Protection Agency. EPA 540-R-97-028.

Box, GEP; Hunter, WG; and Hunter, JS (1978). *Statistics for Experimenters*. John Wiley and Sons, Inc. Printed in the U.S.A.

Bureau of Air Quality Evaluation (2001). *The Summary of Air Quality Modeling Analysis for Particulate Emissions from Southdown Quarry (Now Cemex)"* NJDEP. September 4.

EOHSI – The Environmental and Occupational Health Sciences Institute (2001) *Quality Assurance Project Plan: Assessment of Population Exposure and Risks to Emissions of Protocol Structures and Other Biologically Relevant Structures from the Southdown Quarry*. Prepared for the NJDEP.

Expert Panel-Commissioned by NJDEP/EPA (2000). *Framework for Assessing Possible Risks Posed by the Presence of Asbestos in Marble Mined at the Southdown Quarry in Sussex County, New Jersey.* Prepared for the NJDEP and EPA. March.

Health Effects Institute - Asbestos Research (1991). *Asbestos in Public and Commercial Buildings: A Literature Review and Synthesis of Current Knowledge.* HEI-AR, 141 Portland St., Suite 7100, Cambridge, MA.

International Organization for Standardization (1995). *Ambient Air-Determination of asbestos fibres - Direct-transfer transmission electron microscopy method.* ISO 10312.

Integrated Risk Information System-IRIS (1988). *Toxicological Review of Asbestos.* U.S. Environmental Protection Agency. http://www.epa.gov/iris/subst/0371.htm.

International Agency for Research on Cancer (1977). *Monographs on the Evaluation of Carcinogenic Risks to Man.* Vol 14. IARC, Lyon, France.

Lioy, P; Zhang, J; Freeman, N; Yhn, L; and Hague, R.(2002). *Sparta Township Environmental Asbestos Study. Final Report of the Results of Air and House Dust Sampling.* Prepared for Alan Stern, New Jersey Department of Environmental Protection. October 4.

Lowry, R (2002) Chapter 8 in *Concepts and Applications of Inferential Statistics*, on Web Page of Vasser College. http://faculty.vassar.edu/lowry/webtext.html

NIOSH – National Institute for Occupational Safety and Health (1989). *Method for the determination of asbestos in air using transmission electron microscopy*. NIOSH Method 7402. NIOSH, Cincinnati, Ohio, U.S.A.

NIOSH – National Institute for Occupational Safety and Health (1984). *Method for the Determination of Asbestos in Air Using Phase Contrast Microscopy*. NIOSH Method 7400. NIOSH, Cincinnati, Ohio, U.S.A.

Occupational Safety and Health Administration (1992). "Occupational Exposure to Asbestos, Tremolite, Anthophyllite, and Actinolite; Final Rule." 29 CFR Parts 1910 and 1926. *Federal Register 57:109:24310-24331.* June 8.

Ritter, J. (1998), *Binomial and Poisson Statistics Functions in Java Script*, http://www.ciphersbyritter.com/JAVASCRP/BINOMPOI.HTM

Volkert, RA (1999). *Bedrock Geology and Mineralogy of the Southdown, Inc. (Sparta) Quarry, Sparta, New Jersey.* Department of Environmental Protection, Division of Science, Research, and Technology. New Jersey Geological Survey.

9 FIGURES AND TABLES

TABLES

TABLE 1:
SUMMARY OF RESULTS FROM ANALYSIS OF CORE SAMPLES FROM SOUTHDOWN QUARRY

			Gird		Count		Concentrations (s/ug)		Analytical	Protocol Structures				7402 Structures		
Depth Interval	EMS Sample No.	Weight (ug)	Opening Area (mm2)	No. Grid Openings	Protocol Amphibole	7402 Amphibole	Protocol Amphibole	7402 Amphibole	Sensitivity (s/ug)	Total	Long	True Asbestos	Long Asbestos	Total	Long	True Asbestos
1	216	120	0.0094	342	**3**	0.5	2.994	0.499	0.998	3	1			0.5	0.5	
2	214	120	0.0094	342	**7**	3	6.986	2.994	0.998	7	3	2	2	3	1	
3	203	118	0.0094	348	**6**	3.5	5.984	3.491	0.997	6	2	2	1	3.5		
4	201	110	0.0094	373	**18**	4	17.968	3.993	0.998	18	9	12	5	4	2	2
4	201	110	0.0093	377	12	4	11.979	3.993	0.998	12	7	1	1	4	4	1
4	201	110	0.0095	377	**17**	7	16.613	6.841	0.977	17	12	10	8	7	4	4
4	201D	123	0.0094	350	**13**	9	12.368	8.563	0.951	13	ND	ND	ND	9	ND	ND
5	212	120	0.0094	342	**3**	5	2.994	4.990	0.998	3	1	3	1	5	2	1
6	210	106	0.0097	391	**11**	8	10.534	7.661	0.958	11	2	8	1	8	3	3
6	210	106	0.0096	379	**1**	6	0.998	5.990	0.998	1				6	3	
6	207	104	0.0094	394	**31**	10	30.986	9.995	1.000	31	14	11	8	10	6	
6	207	104	0.0093	407	24	14	23.473	13.692	0.978	24	12	10	4	14	2	5
6	207/210D	114	0.0093	363	47	24	47.018	24.009	1.000	47	16	3	1	24	6.5	1.5
7	209	121	0.0096	332	**1**	0	0.998	0.000	0.998	1				0		
8	208	122	0.0096	329	**1**	1	0.999	0.999	0.999	1				1		
9	217	116	0.0094	354	**0**	1	0.000	0.997	0.997	0	--	--	--	1		
9	205	121	0.0096	332	**1**	2	0.998	1.997	0.998	1	1	1	1	2	1	
9	205	121	0.0096	329	**0**	1	0.000	1.007	1.007	0	--	--	--	1		
9	205	121	0.0096	346	**3**	2	2.874	1.916	0.958	3		3		2		2
9	205/217D	122	0.0094	350	**2**	2	1.918	1.918	0.959	2	ND	ND	ND	2	ND	ND
10	204	110	0.0096	365	**4**	2	3.995	1.998	0.999	4	2	3	2	2	1	1
11	206	100	0.0093	414	**0**	1	0.000	1.000	1.000	0				1		
12	215	111	0.0093	414	**0**	1.5	0.000	1.351	0.901	0				1.5		
13	213	121	0.0093	414	**0**	0	0.000	0.000	0.826	0				0		
14	202	114	0.0093	414	**0**	0	0.000	0.000	0.877	0				0		
15	211	113	0.0093	414	**1**	1	0.885	0.885	0.885	1	1			1		
			Total Structures:		**206**	**112.5**				**206**	**83**	**69**	**35**	**112.5**	**36**	**20.5**
BLANKS:										**% Total:**	**40%**	**33%**	**17%**		**32%**	**18%**
Blank	Blank		0.0094	350	**0**	0										
Lot Blank	Blank		0.0093	414	**0**	0										
Lot Blank	Blank		0.0096	414	**0**	0										

Notes:

Structure numbers presented in this table include only amphibole (tremolite structures).
The one chrysotile protocol structure observed in Sample 201 (0135217HT) is not included above.

Rows shaded in similar colors are replicates or duplicates.

"ND" means not determined.

Blanks reported here do not include sand blanks analyzed by EMS.

TABLE 2:
CORE SAMPLE QUALITY CONTROL PROGRAM COMPONENTS

Activity	Number of Samples	Laboratory
Preparation of Duplicate Splits	3	EMS
Within Laboratory Replicate/Duplicate Analysis	5	RJ Lee
Within Laboratory Replicate/Duplicate Analysis	3	EMS
Between Laobratory Replicate Analysis	3	RJ Lee/EMS
Lot Blanks	2 per lot	RJ Lee/EMS
Sand Blanks	1 after each sample: Analyze 5%	EMS

TABLE 3:
SUMMARY DATA FOR REPLICATES AND DUPLICATES AMONG CORE SAMPLES FROM SOUTHDOWN

Type of Sample		Reporting Date	Depth Interval	EMS ID No.	No Grid Openings	Counts of Observed Structures: Total Structures	Protocol Structures	7402 Structures	Lab	Mass (ug)	Analytical Sensitivity (s/gPM10)	Unique Analysis Identifier
Duplicate A	Replicate	10/24/02	4	201	373	20	18	4	RJ Lee	110	9.98E+05	4AR1a
	Replicate	3/31/03	4	201	377	12 [a]	12 [a]	4	RJ Lee	110	9.98E+05	4AR2a
	Replicate	4/28/03	4	201	377	NA [b]	17	7 [c]	EMS	110	9.90E+05	4AE3a
Duplicate A		10/24/02	4	201D	350	14	13	9	EMS	123	9.51E+05	4BE4b
Duplicate B	T1 Replicate	4/28/03	6	207	407	NA [b]	24	14 [d]	EMS	104	9.70E+05	6AE1a
	T1 Replicate	9/16/02	6	207	394	38	31	13	RJ Lee	104	1.00E+06	6AR2a
	T1 Replicate	7/18/02	6	210	375	6	1	6	RJ Lee	106	1.03E+06	6AR3b
	T1 Replicate	4/28/03	6	210	391	NA [b]	11	8 [e]	EMS	106	9.60E+05	6AE4b
Duplicate B		3/31/03	6	207/210D	363	63	47	24	RJ Lee	114	1.00E+06	6BR5c
Duplicate C	T2 Replicate	9/17/02	9	217	354	1	0	1	RJ Lee	112	1.03E+06	9AR1a
	Replicate	7/16/02	9	205	333	3	1	2	RJ Lee	121	1.02E+06	9AR2b
	T2 Replicate	10/10/02	9	205	329	1	0	1	RJ Lee	121	1.03E+06	9AR3b
	Replicate	4/28/03	9	205	346	NA [b]	3	2 [f]	EMS	121	9.60E+05	9AE4b
Duplicate C		10/21/02	9	205/217D	350	2	2	2	EMS	122	9.59E+05	9BE5c

Notes:

-- Shading highlights true replicate samples (I.e. results from the re-analysis of an identical set of specimen grids).

-- T-Replicates are analyses of paired sets of specimen grids prepared, respectively, from filters collected at different times during the same elutriator run.

-- Duplicates are analyses of paired sets of specimen grids prepared, respectively, from filters collected during separate elutriator runs of duplicate splits from the same samples.

[a] One chrysotile fiber was also observed along with the amphibole structures in this sample. However, it is not included in the structure counts indicated above.

[b] Because EMS completed protocol structure counts and 7402 counts on a different set of grid openings it is not possible to estimate counts of total structures for these samples.

[c] 7402 structures were counted over 381 g.o. for this sample

[d] 7402 structures were counted over 400 g.o. for this sample

[e] 7402 structures were counted over 396 g.o. for this sample

[f] 7402 structures were counted over 350 g.o. for this sample

Table 4:
CHI-SQUARE EVALUATION TO DETERMINE THE COMPARABILITY OF MULTIPLE ANALYSES

Degrees of Freedom	Critical Value	Chi-Square Statistic		Conclusion		Data Set
		Prot Str	7402 Str	Prot Str	7402 Str	
14	23.6	135.37	61.91	**Different**	**Different**	Across all depth intervals (with results averaged across duplicates and replicates)
3	7.81	1.73	3.00	Similar	Similar	Across all duplicates and replicates from Depth Interval 4
4	9.49	5.67	0.75	Similar	Similar	Across all duplicates and replicates from Depth Interval 9
4	9.49	55.65	11.31	**Different**	**Different**	Across all duplicates and replicates from Depth Interval 6
3	7.81	23.89	9.14	**Different**	**Different**	Depth Interval 6, omitting the RJ Lee analysis of Sample No. 210 (omitting Analysis No. 6AR3b)
2	5.99	8.18	4.35	**Different**	Similar	Depth Interval 6, omitting the replicates for Sample No. 210 (omitting Analyses Nos. 6AR3b and 6AR4b)

TABLE 5:
STATISTICAL TESTS FOR COMPARABILITY OF PAIRED ANALYSES

Depth Interval	Sample Analyses Compared		Test Statistic			Conclusions			Comments
			total str	prot str	7402 str	total str	prot str	7402 str	
4	4AR1a	4AR2a	1.414	1.095	0.000	similar	similar	similar	within lab replicate
4	4AR2a	4AE3a		-0.928	-0.905		similar	similar	between lab replicate
4	4AR1a	4BE4c	1.029	0.898	-1.387	similar	similar	similar	between duplicate and lab
4	4AE3a	4BE4c		0.730	-0.500		similar	similar	within lab, between duplicate
6	6AE1a	6AR2a		-0.944	0.192		similar	similar	between lab replicate
6	6AR2a	6AR3b	**4.824**	**5.303**	1.606	**Different**	**Different**	similar	within lab,between T-replicates
6	6AR3b	6AE4b		**-2.887**	-0.535		**Different**	similar	between lab replicate
6	6AE1a	6AE4b		**2.197**	1.279		**Different**	similar	within lab,between T-replicates
6	6AR2a	6BR5c	**-2.488**	-1.812	-1.808	**Different**	similar	similar	within lab, between duplicate
6	6AE1a	6BR5c		**-2.730**	-1.622		**Different**	similar	between duplicate and lab
6	6AR3b	6BR5c	**-6.86199**	**-6.640**	**-3.286**	**Different**	**Different**	**Different**	within lab, between duplicate
6	6AE4b	6BR5c		**-4.727**	**-2.828**	**Different**	**Different**	**Different**	between duplicate and lab
9	9AR1a	9AR2b	-1.000	-1.000	-0.577	similar	similar	similar	within lab,between T-replicates
9	9AR2b	9AR3b	1.000	1.000	0.577	similar	similar	similar	within lab replicate
9	9AR3b	9AE4b		-1.732	-0.577		similar	similar	between lab replicate
9	9AE4b	9BE5c		0.447	0.000		similar	similar	within lab, between duplicate
9	9AR1a	9BE5c	-0.577	-1.414	-0.577	similar	similar	similar	between duplicate and lab

Notes:

Because Poisson Distributions can be approximated as normal distributions with mean zero and standard deviation of 1. The critical value for such a distribution (at the 0.05 level of significance) is 1.96.

Thus, any value of the test statistic greater than 1.96 in the above table suggests a significant difference between the number of structures observed in the indicated analyses.

The test statistic for these comparison is determined as: $(a-b)/(a+b)^{0.5}$ Where a and b are the counts of the number of structures derived, respectively, from each of the two analyses being compared.

TABLE 6:
CHI-SQUARE TESTS TO EVALUATE UNIFORMITY OF DEPOSITS ON ANALYTICAL FILTERS

Unique Analytical Identifier	Depth Interval	Sample Number	Degrees of Freedom	Critical Value	Chi-square Statistic			Conclusions		
					Total Str	Prot Str	7402 Str	Total Str	Prot Str	7402 Str
4AR1a	4	201								
4AR2a	4	201								
4AE3a	4	201	4	9.49	NA	6.24	3.71	NA	Similar	Similar
4BE4b	4	201D	4	9.49	1.00	0.55	6.00	Similar	Similar	Similar
6AE1a	6	207	4	9.49	NA	5.17	8.14	NA	Similar	Similar
6AR2a	6	207	3	7.81	0.32	1.90	2.69	Similar	Similar	Similar
6AR3b	6	210	3	7.81	0.67	3.00	0.67	Similar	Similar	Similar
6AE4b	6	210	4	9.49	NA	5.82	10.75	NA	Similar	**Different**
6BR5c	6	207/210D								
9AR1a	9	217	3	7.81	2.75	ND	2.75	Similar	ND	Similar
9AR2b	9	205	2	5.99	6.00	2.00	4.00	**Different**	Similar	Similar
9AR3b	9	205	3	7.81	2.75	ND	2.75	Similar	ND	Similar
9AR4b	9	205	4	9.49	NA	5.33	3.00	ND	Similar	Similar
9AR5c	9	205/217D	4	9.49	8.00	8.00	8.00	Similar	Similar	Similar

Notes:

NA means not analyzed (because total structures were not determined in the indicated category).
ND means not detected (because no structures were detected in this category)

TABLE 7:
SUMMARY OF RESULTS FROM ANALYSIS OF CORE SAMPLES FROM SOUTHDOWN QUARRY

			Gird		Count		Concentrations (s/ug)		Analytical	Reicprocal	Protocol Structures				7402 Structures		
Depth Interval	EMS Sample No.	Weight (ug)	Opening Area (mm2)	No. Grid Openings	Protocol Amphibole	7402 Amphibole	Protocol Amphibole	7402 Amphibole	Sensitivity (s/ug)	Analytical Sensitivity	Total	Long	True Asbestos	Long Asbestos	Total	Long	True Asbestos
1	216	120	0.0094	342	**3**	0.5	2.994	0.499	0.998	1.0020	3	1			0.5	0.5	
2	214	120	0.0094	342	**7**	3	6.986	2.994	0.998	1.0020	7	3	2	2	3	1	
3	203	118	0.0094	348	**6**	3.5	5.984	3.491	0.997	1.0026	6	2	2	1	3.5		
4	201	110	0.0094	373	**18**	4	17.968	3.993	0.998								
4	201	110	0.0093	377	12	4	11.979	3.993	0.998	1.0195	15.0	9.3	7.7	4.7	6.0	3.3	2.3
4	201	110	0.0095	377	**17**	7	16.613	6.841	0.977								
4	201D	123	0.0094	350	**13**	9	12.368	8.563	0.951								
5	212	120	0.0094	342	**3**	5	2.994	4.990	0.998	1.0020	3	1	3	1	5	2	1
6	210	106	0.0097	391	**11**	8	10.534	7.661	0.958								
6	210	106	0.0096	379	**1**	6	0.998	5.990	0.998								
6	207	104	0.0094	394	**31**	10	30.986	9.995	1.000	1.0137	22.8	8.8	6.4	2.8	12.4	4.1	1.9
6	207	104	0.0093	407	24	14	23.473	13.692	0.978								
6	207/210D	114	0.0093	363	47	24	47.018	24.009	1.000								
7	209	121	0.0096	332	**1**	0	0.998	0.000	0.998	1.0017	1				0		
8	208	122	0.0096	329	**1**	1	0.999	0.999	0.999	1.0008	1				1		
9	217	116	0.0094	354	**0**	1	0.000	0.997	0.997								
9	205	121	0.0096	332	**1**	2	0.998	1.997	0.998								
9	205	121	0.0096	329	**0**	1	0.000	1.007	1.007	1.0167	1.2	0.2	0.8	0.2	1.6	0.2	0.4
9	205	121	0.0096	346	**3**	2	2.874	1.916	0.958								
9	205/217D	122	0.0094	350	**2**	2	1.918	1.918	0.959								
10	204	110	0.0096	365	**4**	2	3.995	1.998	0.999	1.0011	4	2	3	2	2	1	1
11	206	100	0.0093	414	**0**	1	0.000	1.000	1.000	1.0001	0				1		
12	215	111	0.0093	414	**0**	1.5	0.000	1.351	0.901	1.1101	0				1.5		
13	213	121	0.0093	414	**0**	0	0.000	0.000	0.826	1.2101	0				0		
14	202	114	0.0093	414	**0**	0	0.000	0.000	0.877	1.1401	0				0		
15	211	113	0.0093	414	**1**	1	0.885	0.885	0.885	1.1301	1	1			1		
			Total Structures:		**206**	**112.5**				**Total Structures:**	**65**	**28.3**	**24.9**	**13.7**	**38.5**	**12.1**	**6.6**
										Percent of Total:		**43.6%**	**38.3%**	**21.0%**		**31.5%**	**17.2%**
									Pooled Analytical Sensitivity:	**0.0639**							

Notes:

Structure numbers presented in this table include only amphibole (tremolite structures).
The one chrysotile protocol structure observed in Sample 201 (0135217HT) is not included above.

Rows shaded in similar colors are replicates or duplicates.

TABLE 8:
ESTIMATED EXPOSURES AND THEIR CORRESPONDING RISKS TO NEIGHBORING RESIDENTS POSED BY EMISSIONS OF PROTOCOL STRUCTURES FROM SOUTHDOWN QUARRY

Location of Estimated Maximum Annual Average Concentrations	Modeled Dust Concentrations (ug/M^3)	Protocol Structures			Protocol Structures (True Asbestos fibers Only)		
		Estimated Concentations[1]		Equivalent Risk	Estimated Concentations[1]		Equivalent Risk
		(s/M^3)	(s/cm^3)		(s/M^3)	(s/cm^3)	
Point of Maximum Impact	45	8.2E+01	8.2E-05	**5.E-04**	3.9E+01	3.9E-05	**3.E-04**
at the North Facility Boundary	15	2.7E+01	2.7E-05	**2.E-04**	1.3E+01	1.3E-05	**9.E-05**
at the South FacilityBoundary	4	7.2E+00	7.2E-06	**5.E-05**	3.5E+00	3.5E-06	**2.E-05**
at the Nearest Residence	< 1	1.8E+00	1.8E-06	**< 1.E-05**	8.7E-01	8.7E-07	**< 6.E-06**

Notes:

[1] Concentrations provided are based on weighted protocol structure counts (see text).

TABLE 9:
ESTIMATED EXPOSURES AND THEIR CORRESPONDING RISKS TO NEIGHBORING RESIDENTS POSED BY EMISSIONS OF 7402 STRUCTURES FROM SOUTHDOWN QUARRY

Location of Estimated Maximum Annual Average Concentrations	Modeled Dust Concentrations (ug/m^3)	7402 Structures Estimated Concentations (s/m^3)	7402 Structures Estimated Concentations (s/cm^3)	7402 Structures Equivalent Risk	7402 Structures (True Asbestos Fibers Only) Estimated Concentations (s/m^3)	7402 Structures (True Asbestos Fibers Only) Estimated Concentations (s/cm^3)	7402 Structures (True Asbestos Fibers Only) Equivalent Risk
Point of Maximum Impact	45	1.1E+02	1.1E-04	**3.E-05**	1.9E+01	1.9E-05	**4.E-06**
at the North Facility Boundary	15	3.7E+01	3.7E-05	**8.E-06**	6.4E+00	6.4E-06	**1.E-06**
at the South FacilityBoundary	4	9.8E+00	9.8E-06	**2.E-06**	1.7E+00	1.7E-06	**4.E-07**
at the Nearest Residence	< 1	2.5E+00	2.5E-06	**< 6.E-07**	4.2E-01	4.2E-07	**< 1.E-07**

TABLE 10:
ADDITIONAL RISK PER ONE HUNDRED THOUSAND PERSONS FROM LIFETIME CONTINUOUS EXPOSURE TO 0.0005 TEM f/cc LONGER THAN 5.0 µm AND THINNER THAN 0.5 µm

Receptor Category	Percent of Fibers Greater Than 10 ∝m in Length										
	0	0.05	0.10	0.50	1.00	2.00	5.00	10.00	20.00	50.00	100.00
						CHRYSOTILE					
MALE NON-SMOKERS											
Lung Cancer	0.011	0.013	0.015	0.030	0.05	0.09	0.20	0.39	0.77	1.91	3.81
Mesothelioma	0.004	0.005	0.005	0.011	0.02	0.03	0.07	0.14	0.27	0.67	1.33
Combined	0.015	0.018	0.021	0.041	0.07	0.12	0.27	0.53	1.04	2.58	5.14
FEMALE NON-SMOKERS											
Lung Cancer	0.008	0.010	0.011	0.022	0.04	0.06	0.14	0.28	0.55	1.37	2.74
Mesothelioma	0.004	0.005	0.006	0.012	0.02	0.03	0.08	0.15	0.30	0.74	1.48
Combined	0.013	0.015	0.017	0.034	0.05	0.10	0.22	0.43	0.85	2.11	4.22
MALE SMOKERS											
Lung Cancer	0.097	0.112	0.128	0.256	0.42	0.74	1.70	3.29	6.49	16.08	32.06
Mesothelioma	0.003	0.003	0.004	0.007	0.01	0.02	0.05	0.09	0.18	0.45	0.90
Combined	0.099	0.116	0.132	0.264	0.43	0.76	1.74	3.39	6.67	16.53	32.96
FEMALE SMOKERS											
Lung Cancer	0.067	0.078	0.089	0.178	0.29	0.51	1.18	2.29	4.51	11.18	22.29
Mesothelioma	0.004	0.005	0.005	0.011	0.02	0.03	0.07	0.14	0.27	0.66	1.32
Combined	0.071	0.083	0.095	0.189	0.31	0.54	1.25	2.42	4.78	11.84	23.61
						AMPHIBOLE					
MALE NON-SMOKERS											
Lung Cancer	0.04	0.05	0.05	0.11	0.17	0.31	0.71	1.37	2.70	6.68	13.26
Mesothelioma	2.01	2.34	2.67	5.33	8.65	15.30	35.24	68.45	134.83	333.61	663.65
Combined	2.047	2.386	2.725	5.437	8.83	15.61	35.94	69.82	137.53	340.28	676.91
FEMALE NON-SMOKERS											
Lung Cancer	0.03	0.03	0.04	0.08	0.13	0.22	0.52	1.00	1.98	4.89	9.71
Mesothelioma	2.23	2.60	2.97	5.92	9.61	16.99	39.12	75.99	149.68	370.33	736.66
Combined	2.257	2.631	3.005	5.995	9.73	17.21	39.64	77.00	151.66	375.22	746.37
MALE SMOKERS											
Lung Cancer	0.38	0.45	0.51	1.02	1.66	2.93	6.75	13.12	25.84	63.91	127.06
Mesothelioma	1.36	1.58	1.81	3.61	5.86	10.35	23.84	46.32	91.23	225.72	449.00
Combined	1.742	2.031	2.319	4.628	7.51	13.29	30.60	59.44	117.08	289.63	576.06
FEMALE SMOKERS											
Lung Cancer	0.27	0.32	0.36	0.72	1.17	2.07	4.76	9.25	18.23	45.10	89.70
Mesothelioma	1.98	2.31	2.64	5.27	8.55	15.12	34.83	67.66	133.27	329.68	655.65
Combined	2.255	2.628	3.002	5.989	9.72	17.19	39.59	76.92	151.50	374.78	745.35

Source: Berman and Crump (2001)

FIGURES

Figure 1:

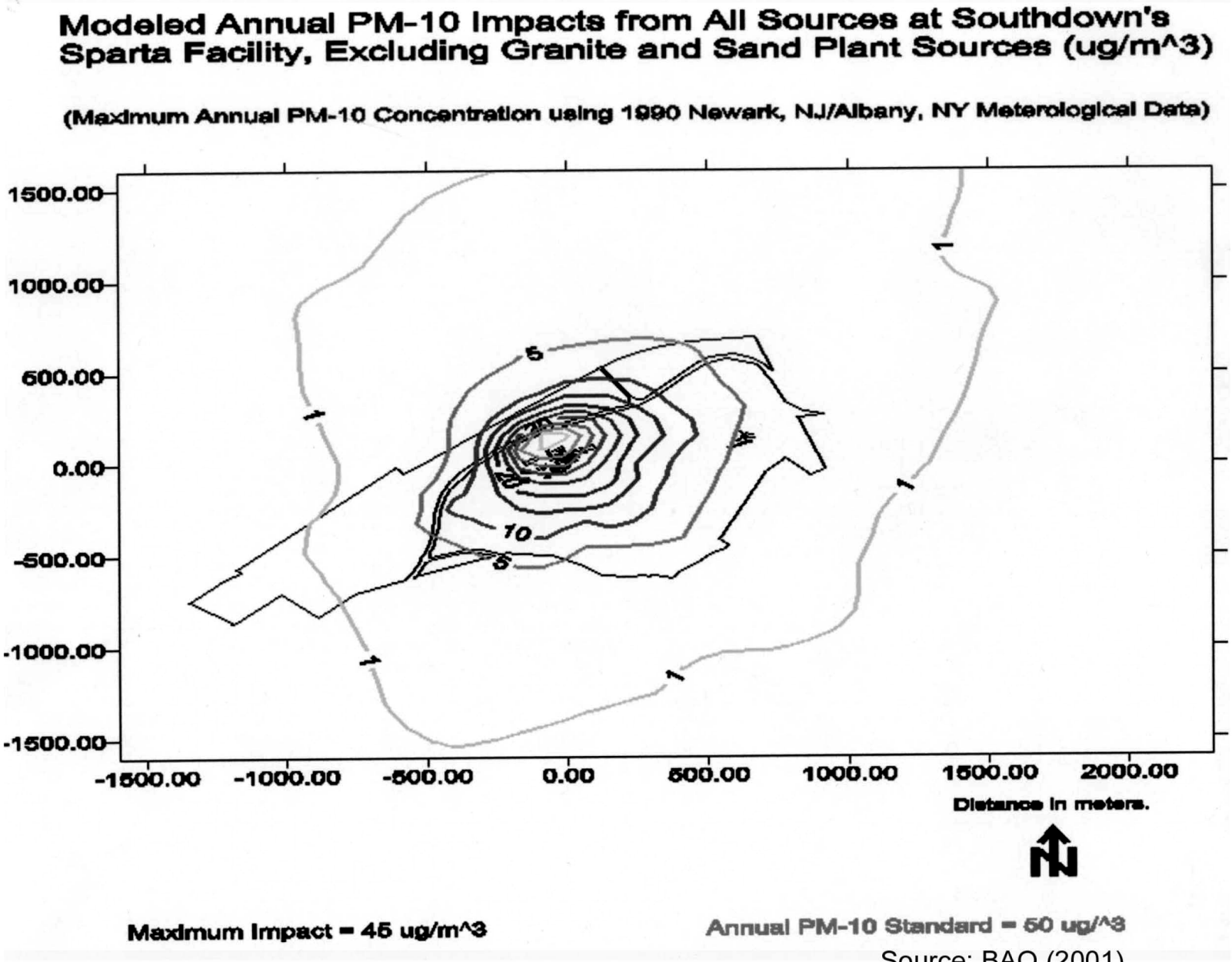

Source: BAQ (2001)

Figure 2:
Photomicrograph of Tremolite Asbestos from Southdown Quarry
Observed Following Dissolution of Marble
(Magnification: 240x at 4 inch reproduction)

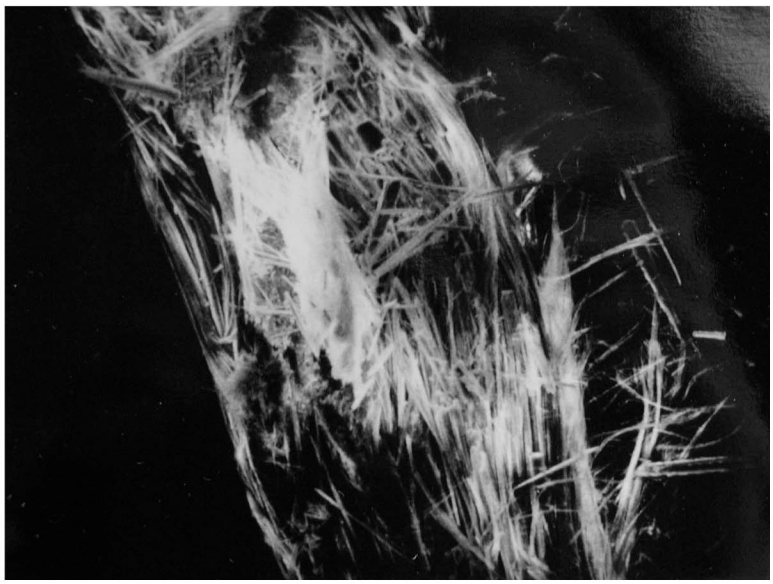

APPENDIX A:
RJ Lee Procedure for Distinguishing Cleavage Fragments from Asbestiform Fibers

Asbestiform fibers are defined as those exhibiting characteristics of: a) high aspect ratios (usually 20:1 to 100:1 or higher), b) curvature, and c) fiber bundles with splayed ends. Asbestiform fibers can occur in bundles of parallel fibers or in matted masses of fibers and fiber bundles. Typically, individual fibers have width dimensions of less than 0.5 μm.

To properly classify a mineral particle as asbestiform or as cleavage, the fiber is examined in the transmission electron microscope. The following simplified flowchart can be used to classify the particle as asbestiform or as cleavage.

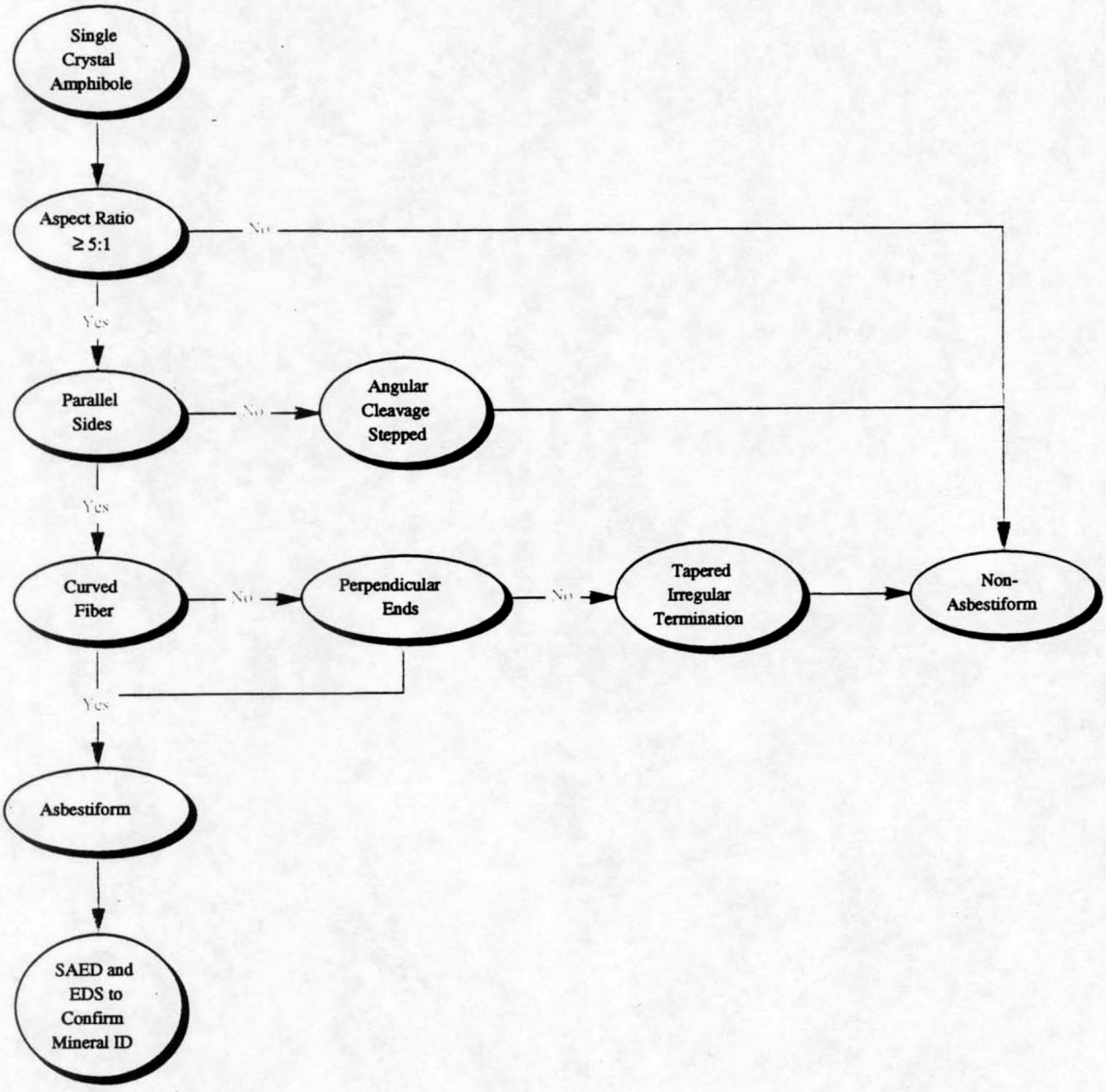

However, for some mineral particles, a more complex scheme (as shown in the next flowchart) is needed to determine asbestiform/cleavage. This second flowchart incorporates additional analyses particularly

useful on amphibole particles. It retains the conservative aspect ratio of the first flowchart (≥ 5:1) but incorporates additional steps such as examining the particle for internal diffraction contours.